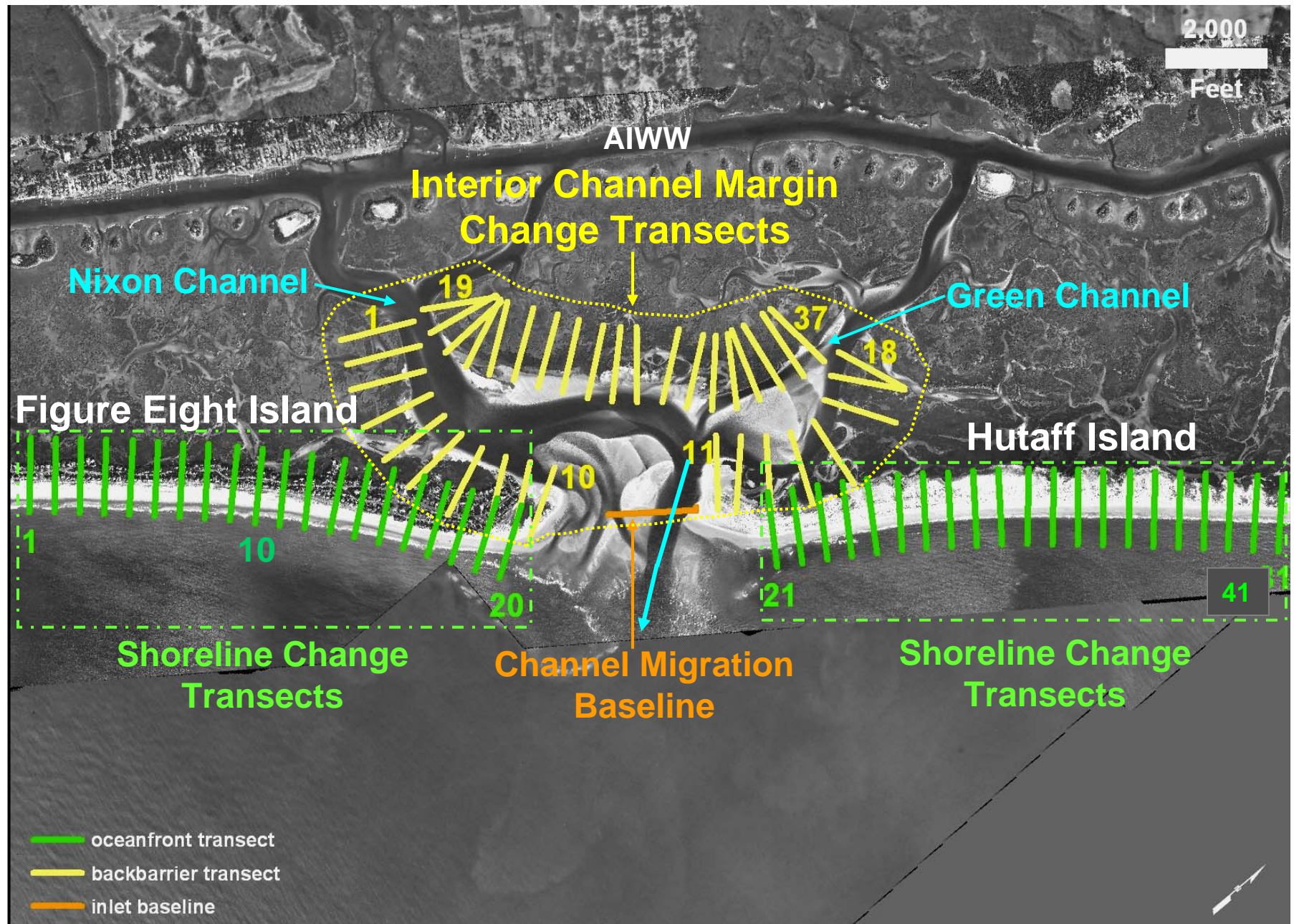


**Figure 1.** Aerial photograph of Rich Inlet, Figure Eight Island and Hutaft Island depicting conditions as of 11/9/08. Note the expansive marginal flood channel located on the F8I margin that acts as a corridor for the transport of large volumes of sand into the estuary and interior channels. Also note the developing spit along the F8I inlet shoreline. Photograph courtesy of GBA- Wilmington, NC.





**Figure 2.** Aerial mosaic (2006) depicting the ebb channel baseline position and the estuarine and oceanfront shoreline transect locations.



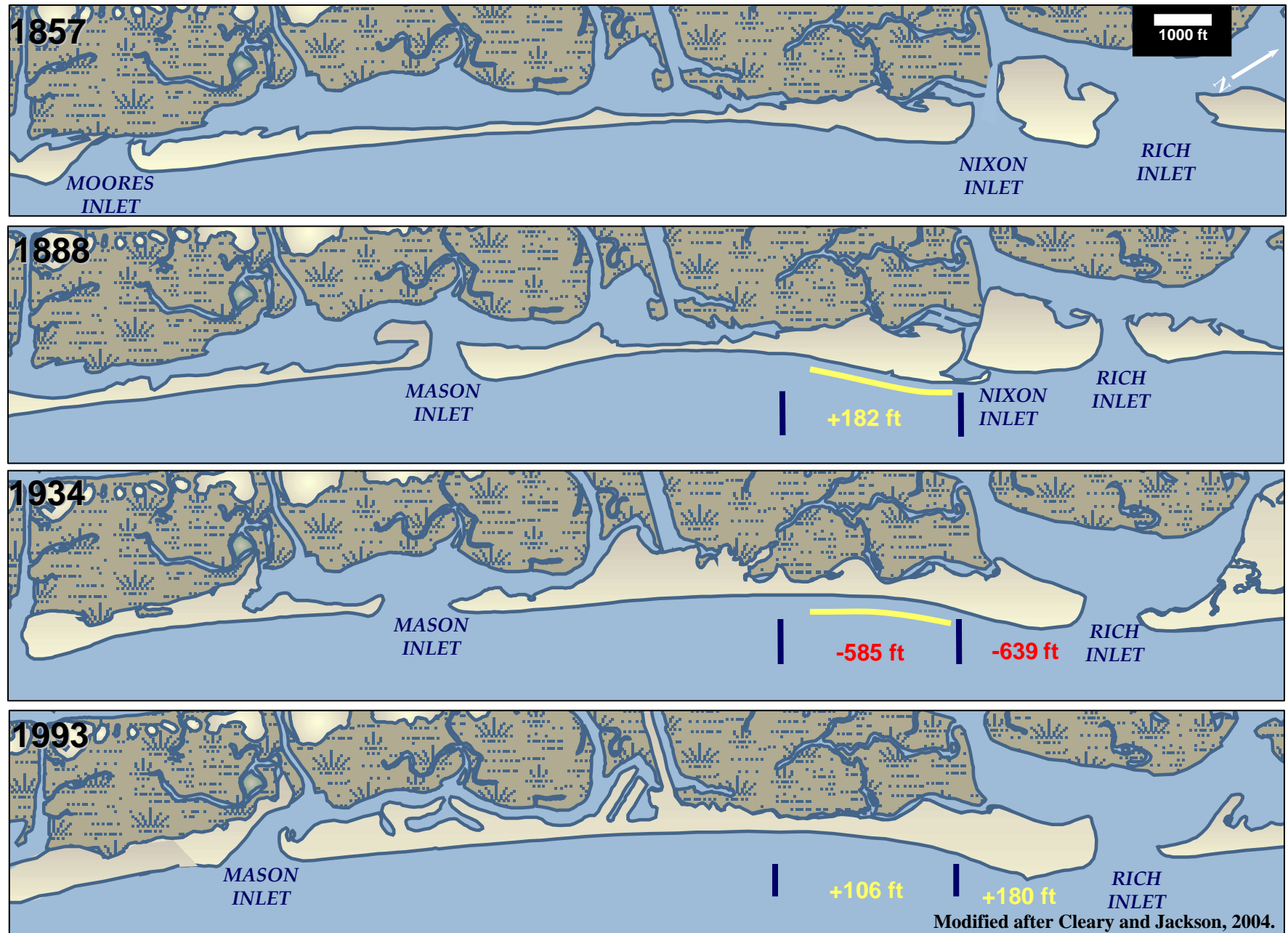


**Figure 3.** Cartoon based on historic maps and a 1993 aerial photograph depicting position of historic Nixon Inlet along the northern portion of F8I. Note the large bulbous shape of the shoreline (yellow line) with the northward extending spit imaged on the 1888 map. By 1934 the incorporated shoreline segment eroded an average of 585 ft while the shoreline reach nearest the inlet eroded an average of 639 ft since inlet closure. Since 1934 the two reaches have prograded an average that ranged from 106 to 180 ft.



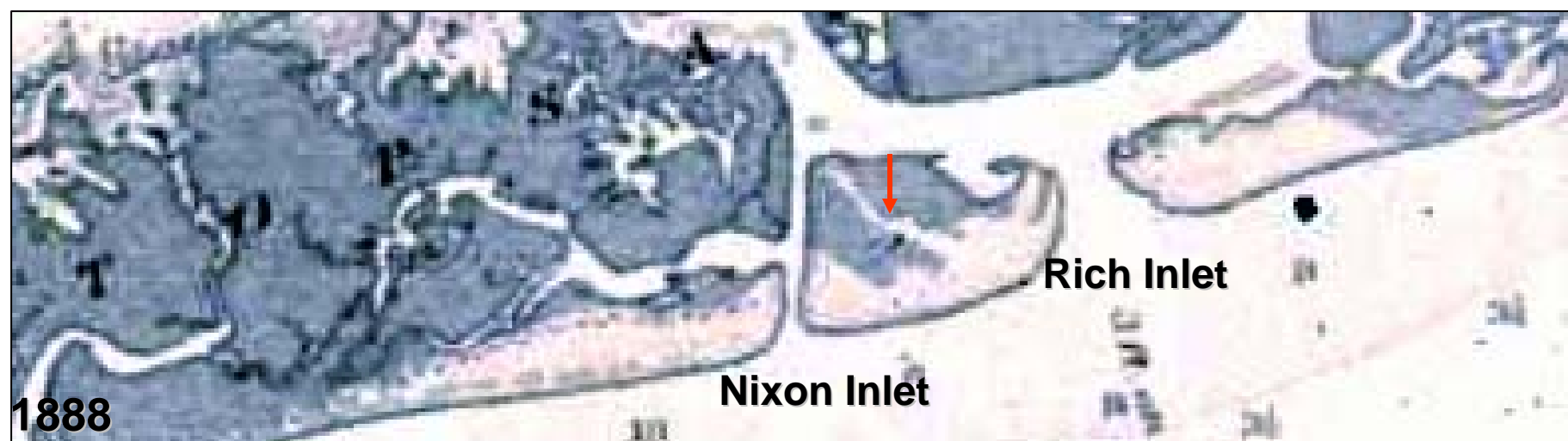
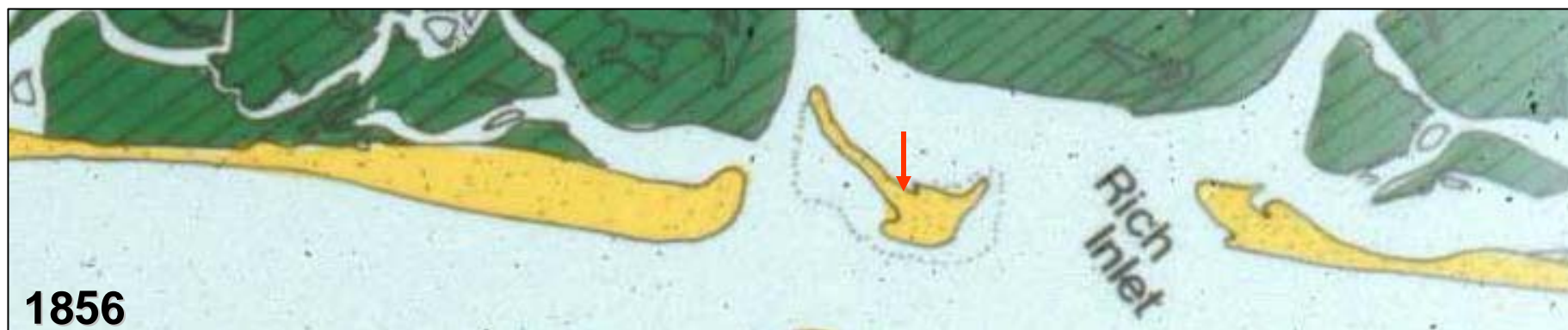
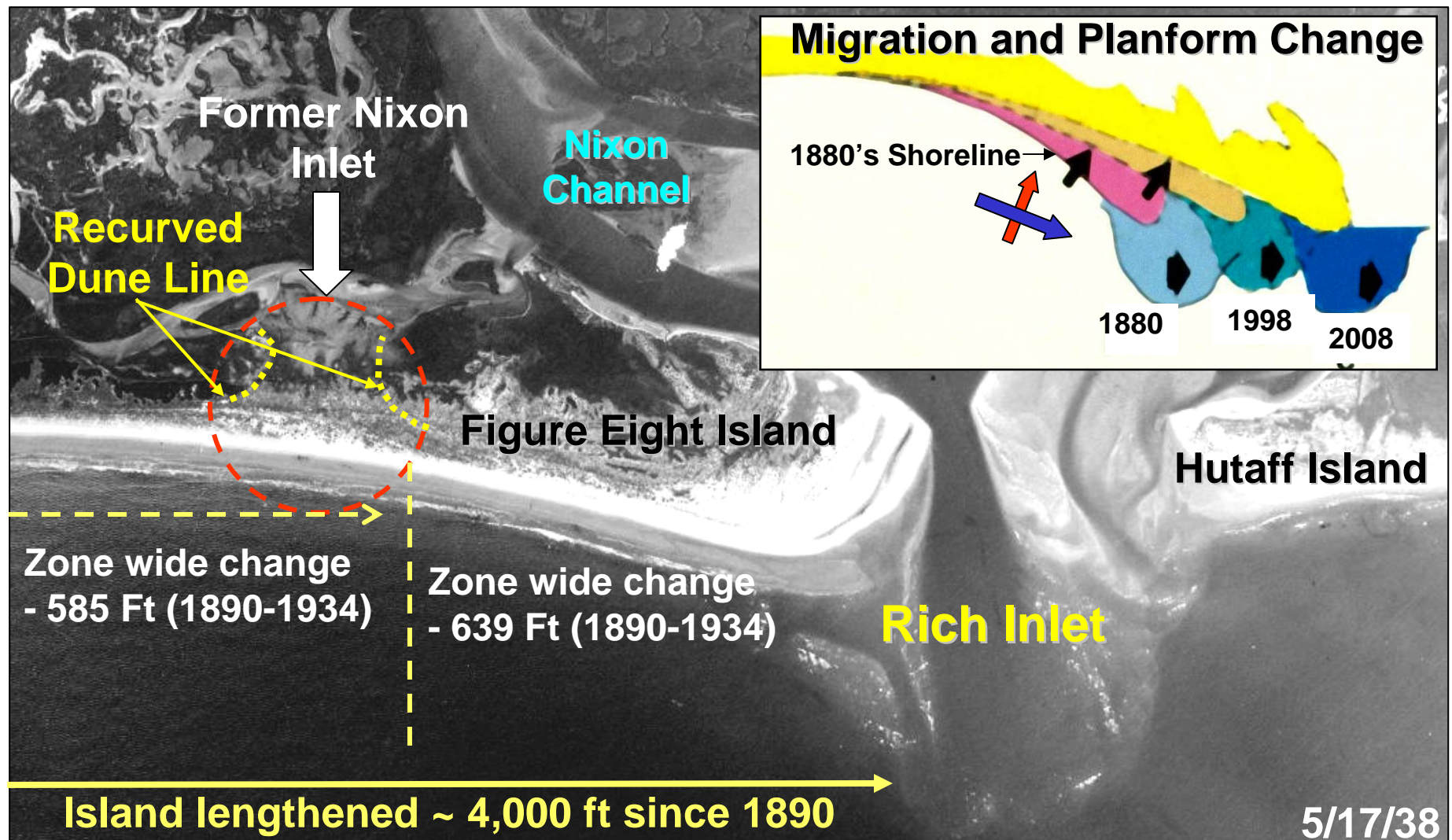


**Figure 4.** Cartoon depicting position of historic Nixon and Rich inlets along the northern portion of F8I in 1856 and 1888. Arrows delineate morphologic features imaged on an 1938 aerial photograph.





5/17/38

**Figure 5.** Historic aerial photograph (1938) depicting the historic late 19<sup>th</sup> C. position of Nixon Inlet and the inlet shoreline features. Insert depicts shoreline planform changes that occurred subsequent to the closure of Nixon Inlet and the attendant lengthening of F8I. Shoreline erosion along the northern portion of the island averaged 585 to 639 ft. See Figure 4 for morphologic features preserved and indentified on 1938 photograph. Modified after Cleary and Jackson 2004.



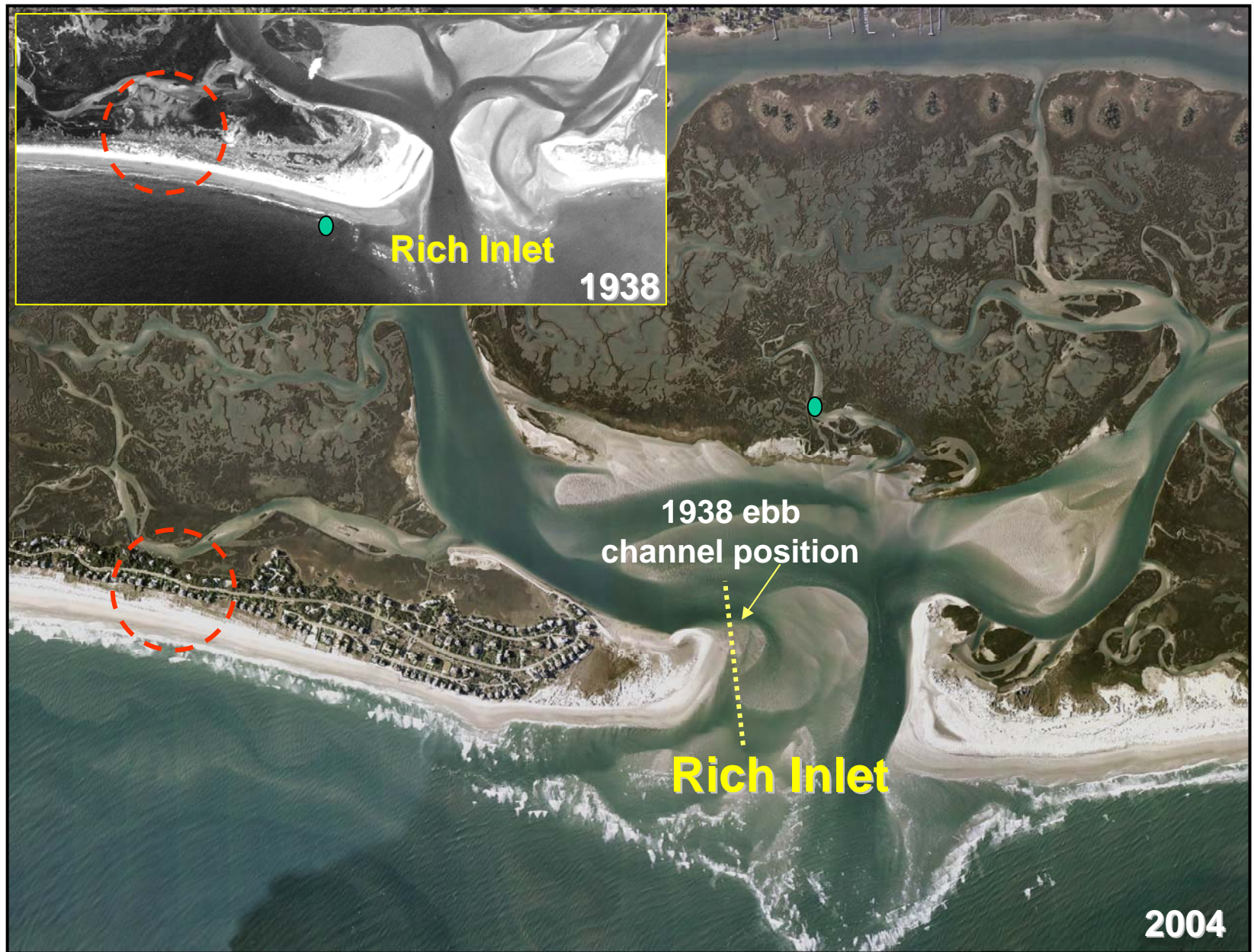


**Figure 6.** Recent aerial photograph (2004) depicting the location of historic Nixon Inlet and the shoreline conditions downdrift of Rich Inlet. Insert is a 1938 photograph of the area and the location of Nixon Inlet and the bulbous shape of the shoreline downdrift of Rich Inlet.



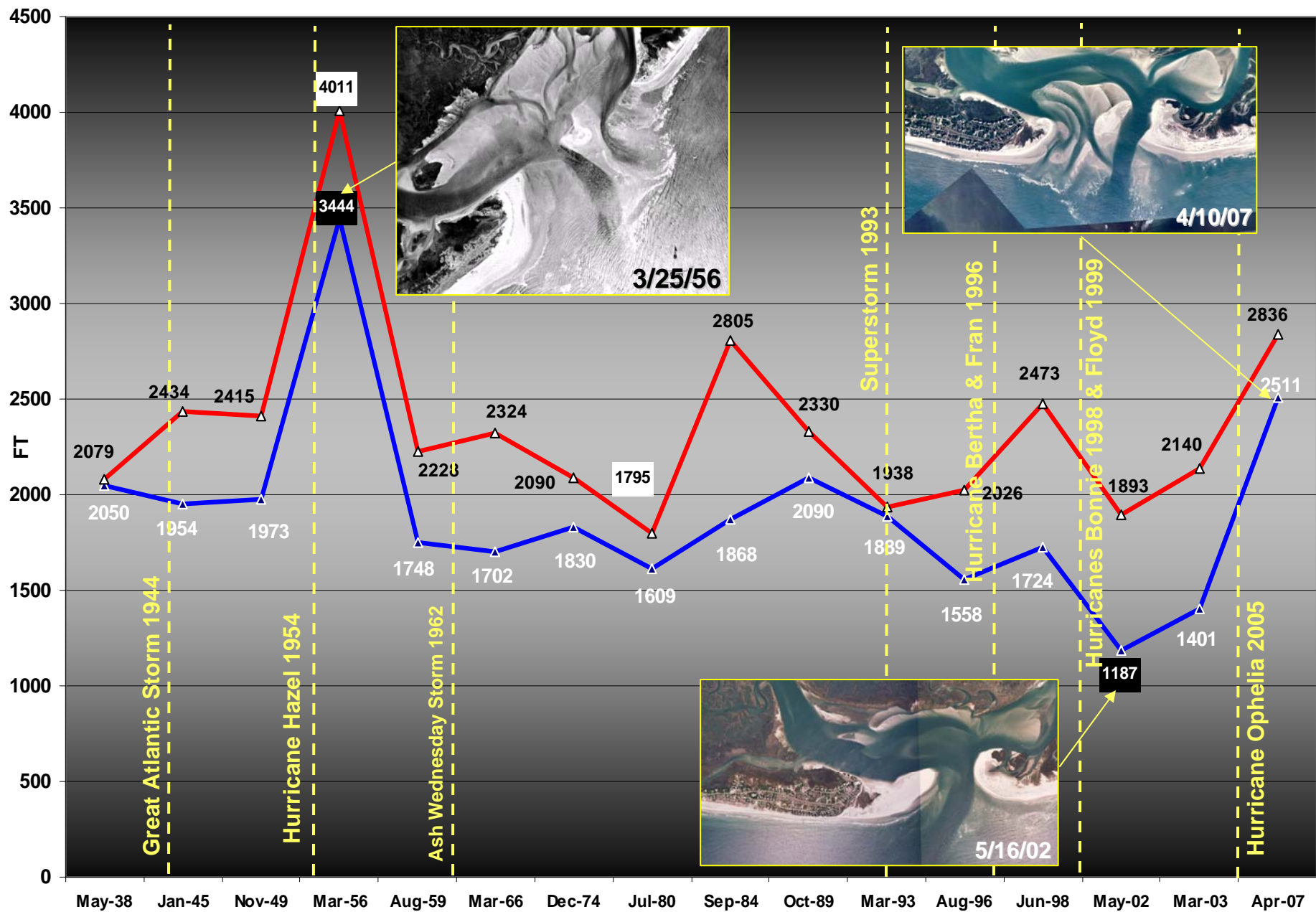


**Figure 7.** Line graphs depicting the inlet's minimum width (IMW) and baseline width since 1938. See Figure 2 for location of inlet baseline. The inserts are historical aerial photographs that depict the current (2007) and minimum (2002) IMW as well as the storm-related widening of the inlet (3/25/56) due to Hurricane Hazel in October 1954.

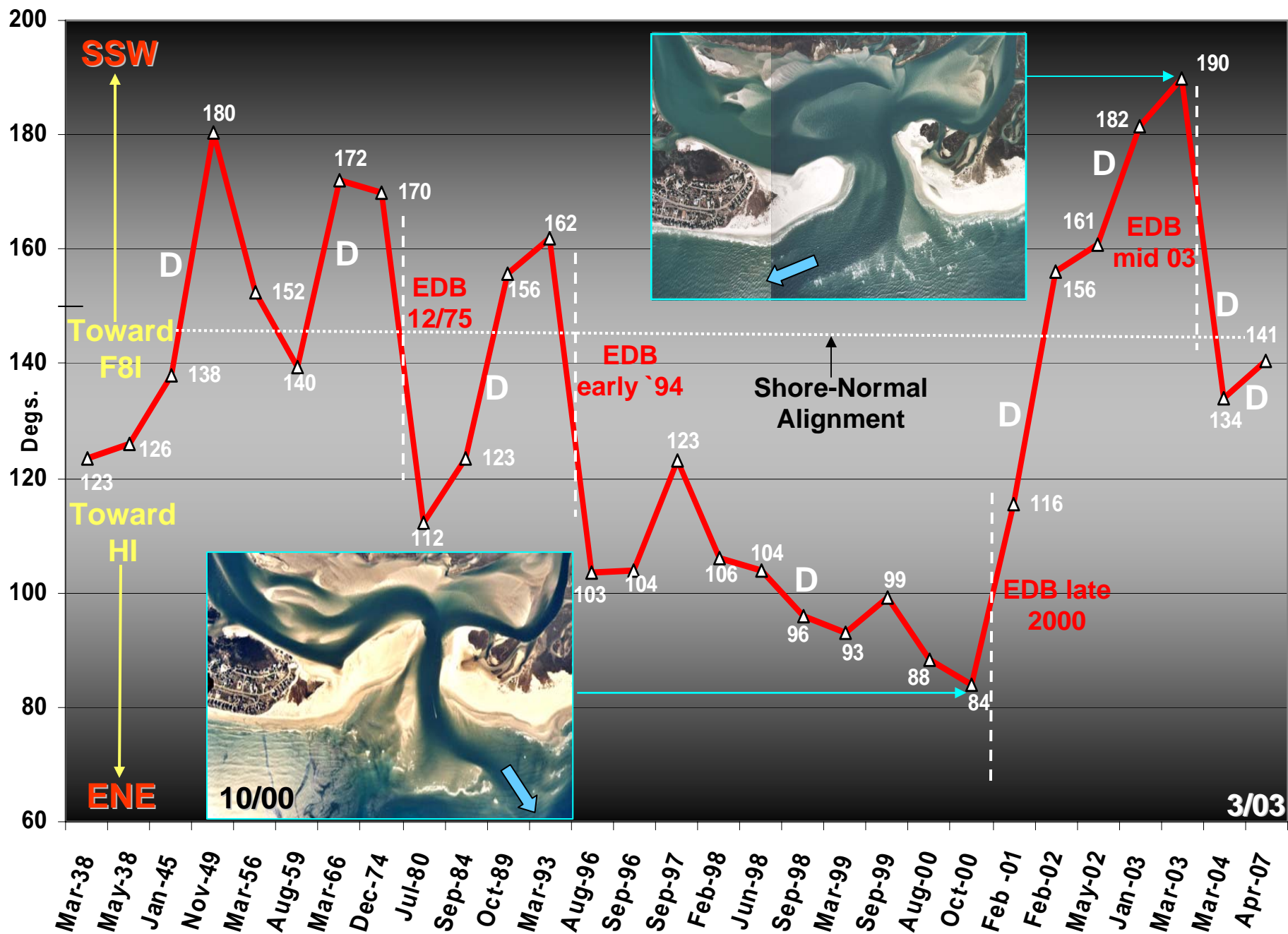


**Figure 8.** Line graph depicting the orientation (azimuth) of the outer portion of the ebb channel since 1938. The inserts are historical aerial photographs that depict the maximum (2003) and minimum (2000) azimuths of the ebb channel. Ebb delta breaching events that occurred between 1938 and 2007 are labeled “EDB” while channel deflection is labeled by a white colored “D”.



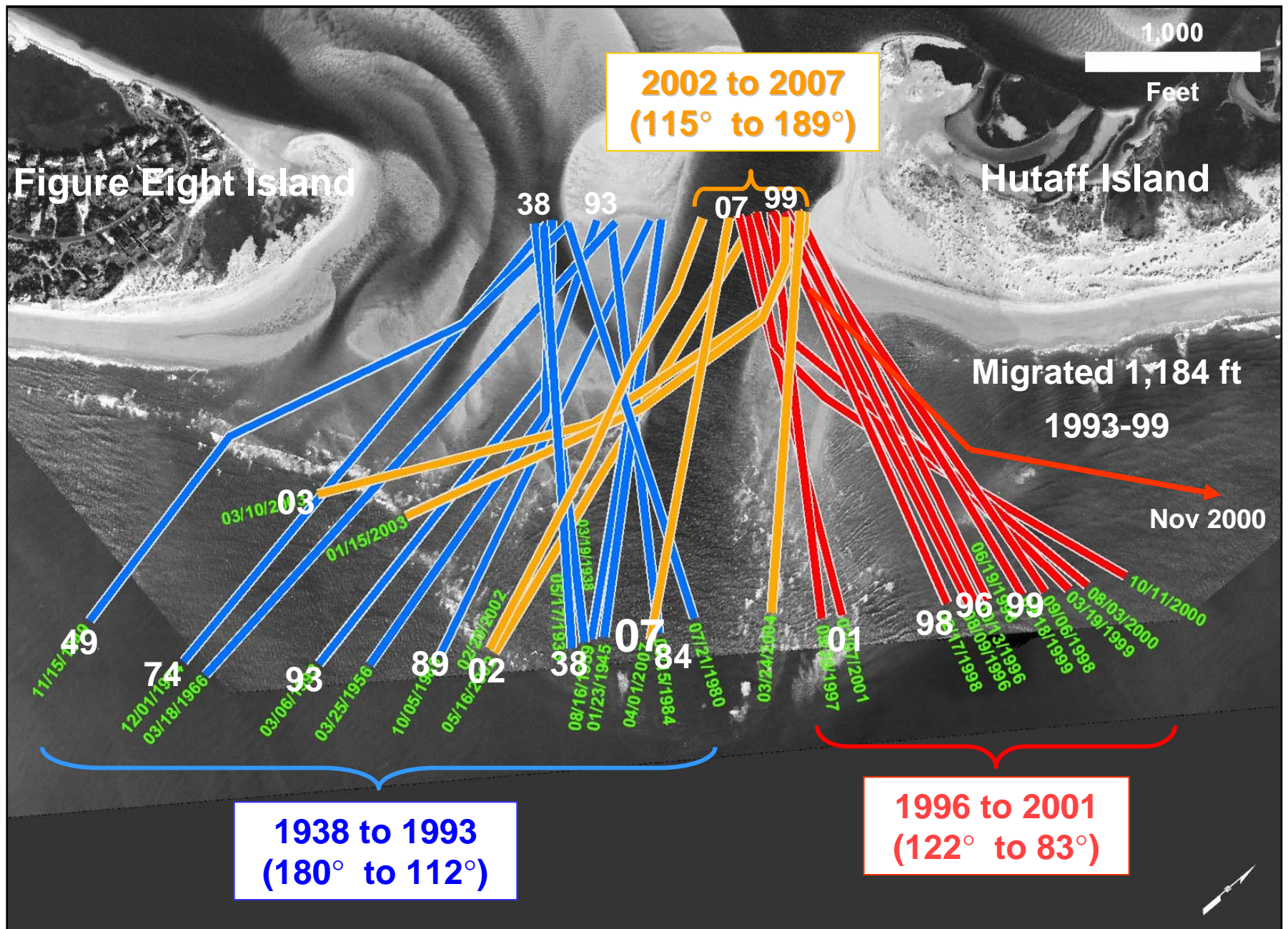


**Figure 9.** Aerial photograph mosaic (2006) depicting position of the ebb channel between 1938 and 2007. During the mid 1990s the ebb channel shifted to the NE ~1,184 ft and has remained in same general location. Note the changing alignment of outer portion of the ebb channel.

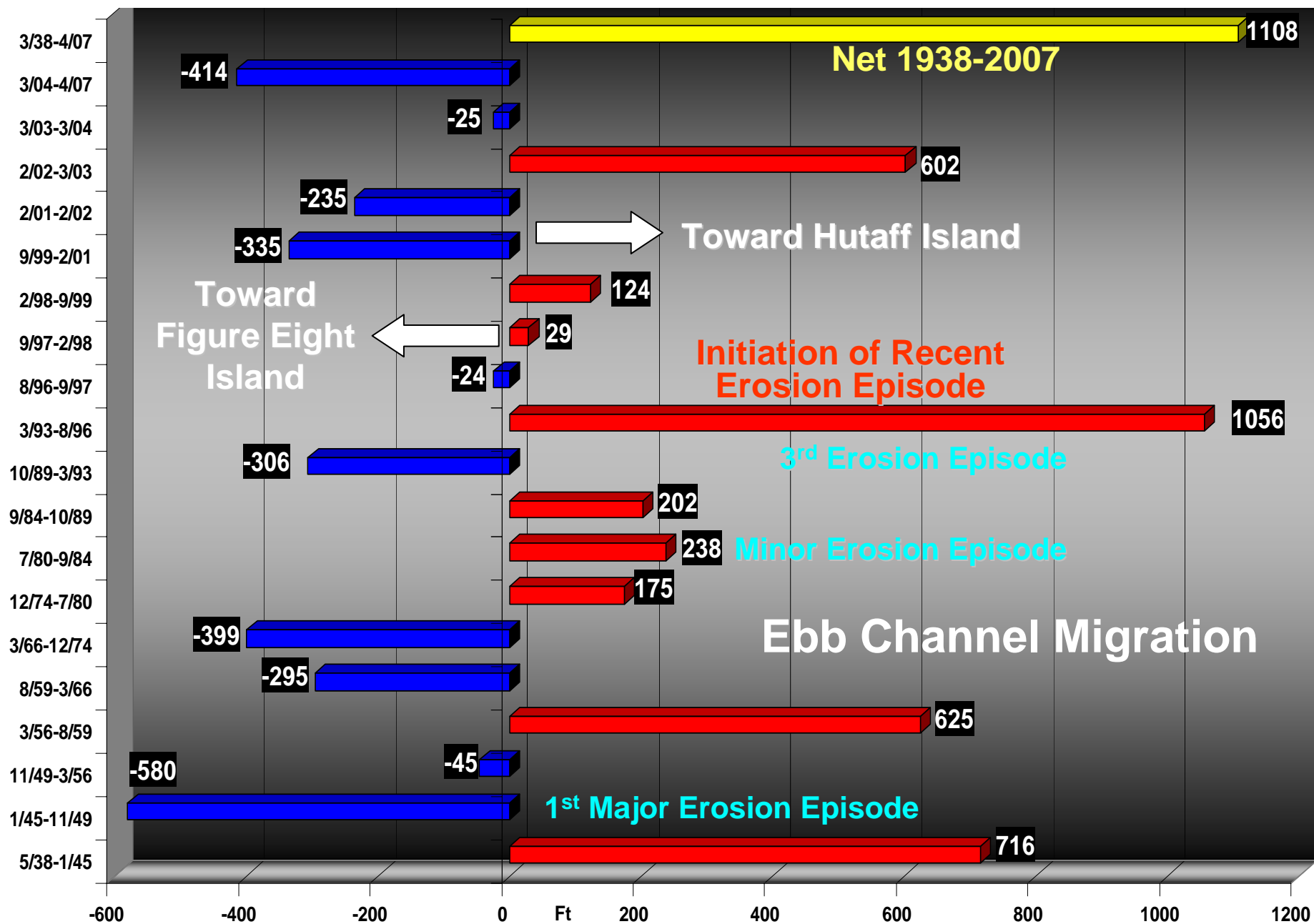


**Figure 10.** Bar graph depicting migration of Rich's Inlet ebb channel (throat segment) between March 1938 and April 2007.



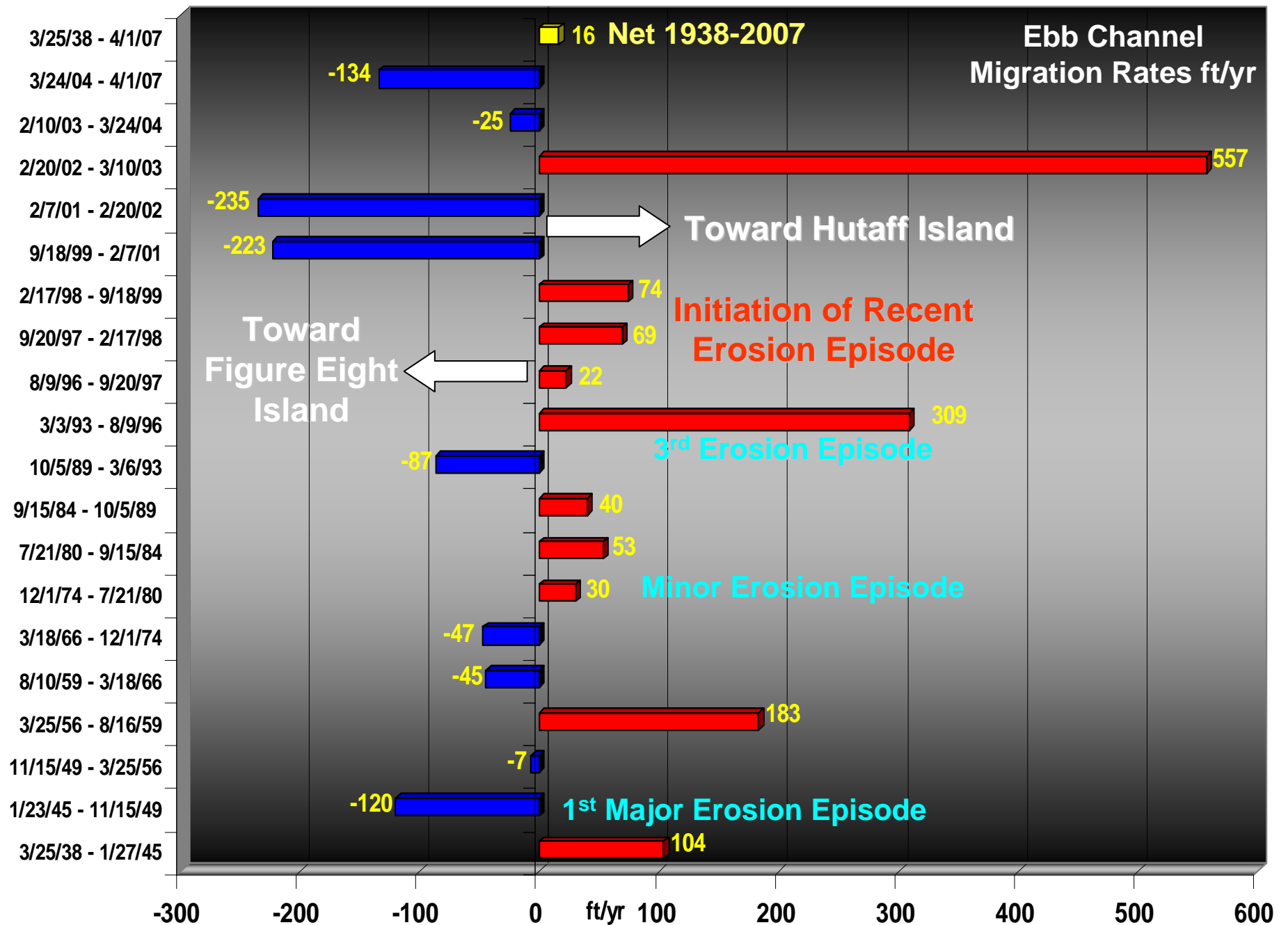


**Figure 11.** Graph depicting ebb channel migration rates for various time intervals between 1938 and 2007.

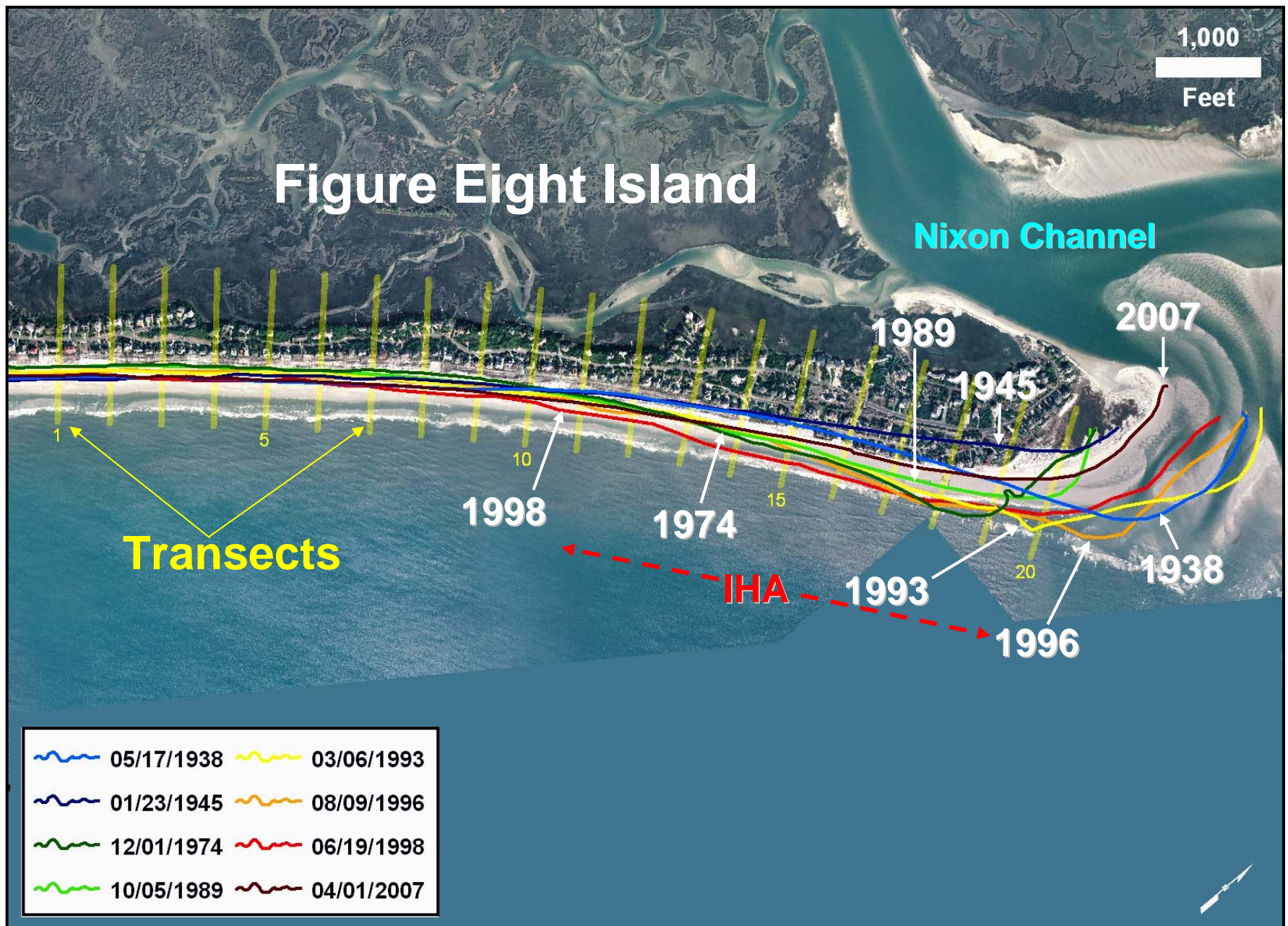


**Figure 12.** Aerial photograph (2007) depicting selected (8) shoreline positions along F8I since 1938 and transect locations (T1-20). The F8I Rich Inlet IHA includes the shoreline reach between Transects 11 and 20. Note that the 1945 shoreline position is the most landward positioned shoreline. Also note a significant number of homes lie seaward of the 1945 shoreline position



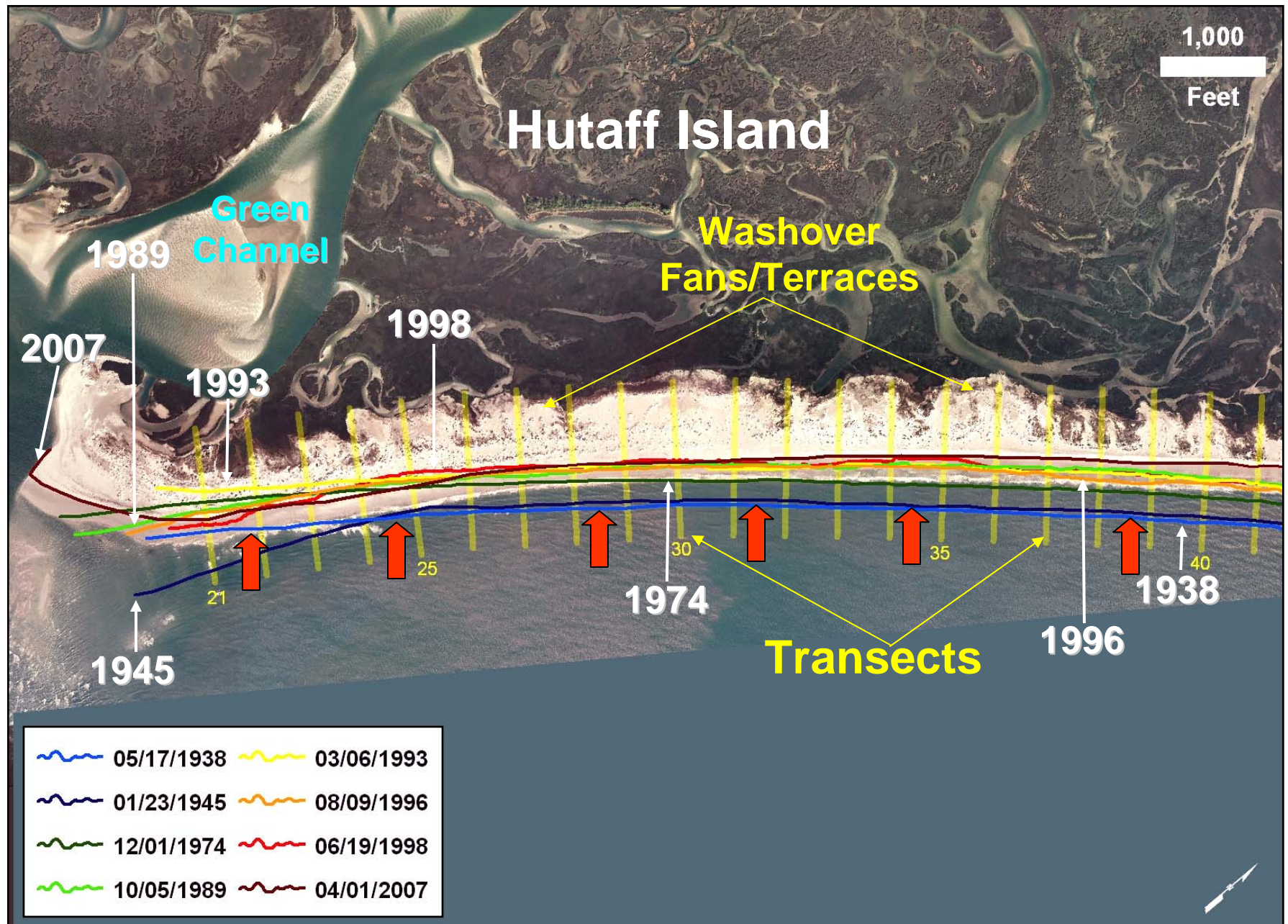


**Figure 13.** Aerial photograph (2007) depicting selected (8) shoreline positions along HI since 1938 and transect locations (T21-41). The entirety of Hutaff Island is included within an IHA. For purposes of comparison and discussion this study has designated the Rich Inlet zone of influence to include the shoreline reach between Transect 21 and 30. Note that the relative positions of the 1938 and 1945 shorelines along the barrier. Also note the continuous retreat of the shoreline since 1938 north of T 26.

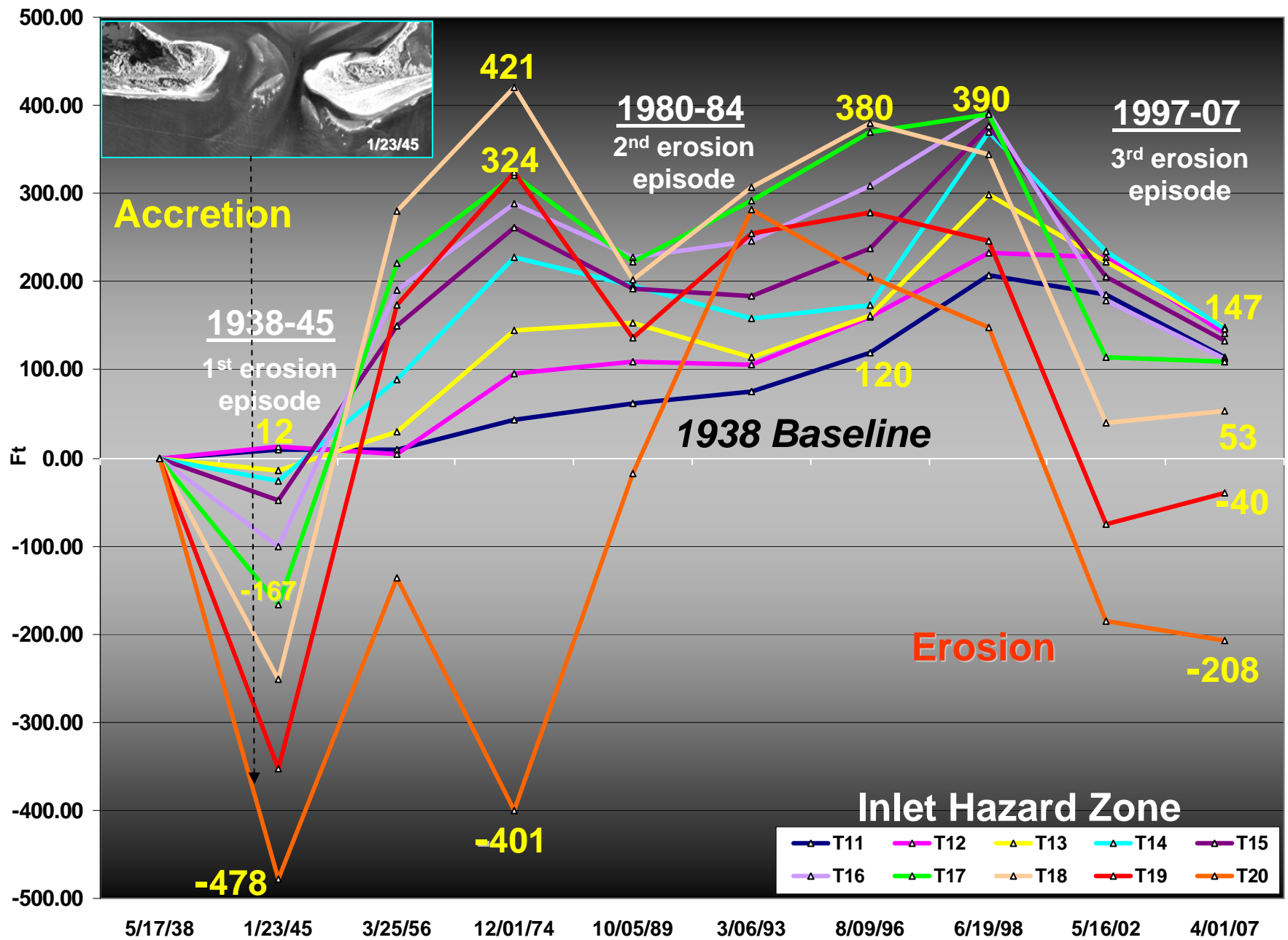


**Figure 14.** Graph depicting the cumulative shoreline change along transects located within the IHA (T11 to T20) on F8I. Photograph inserts depict condition of the shoreline during the 1<sup>st</sup> erosion episode.



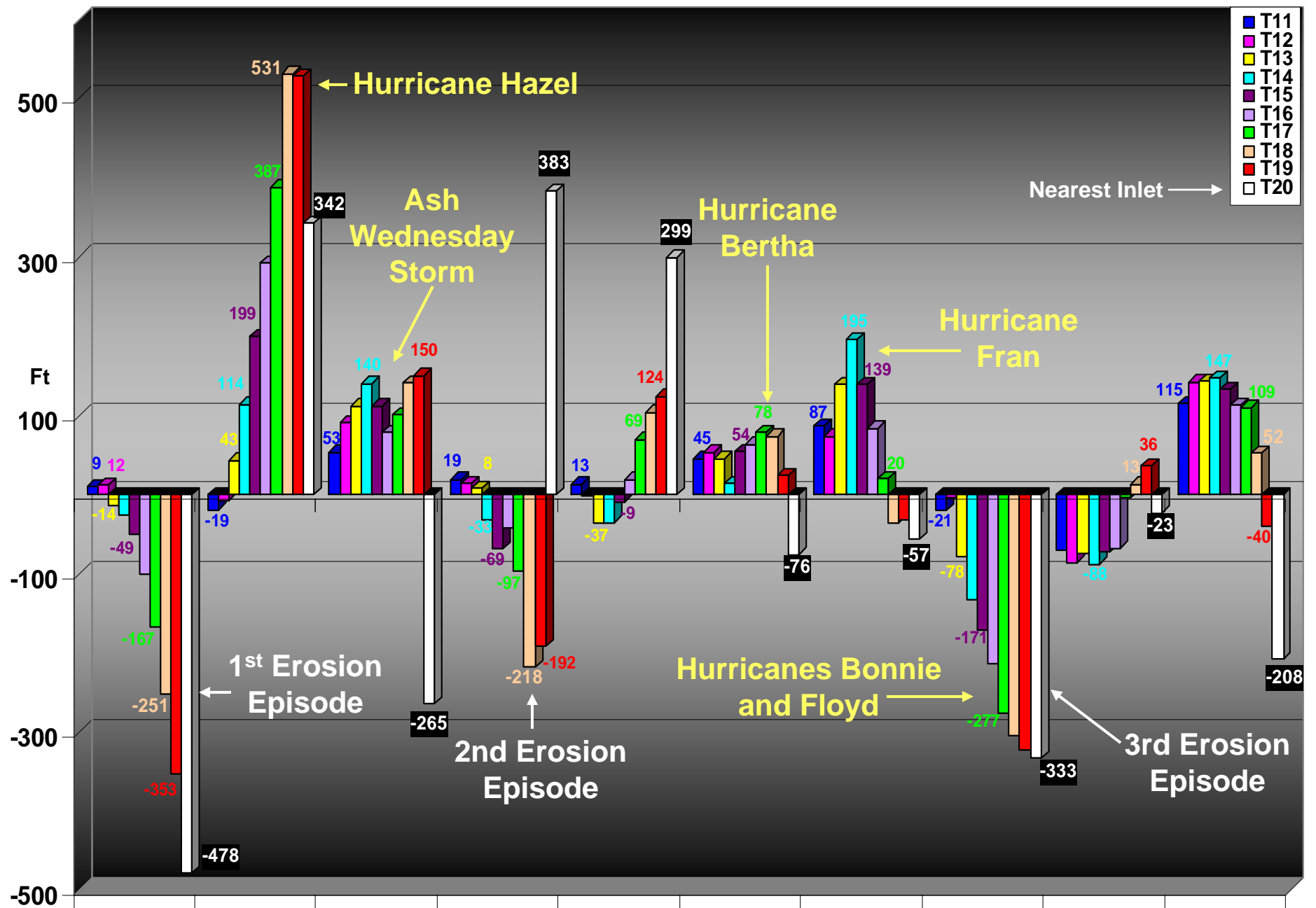


**Figure 15.** Bar graph depicting short-term shoreline changes along the oceanfront between the T11 and T 20 from 1938 to 2007. The oceanfront shoreline segment lies within the F8I portion of the Rich Inlet IHA.

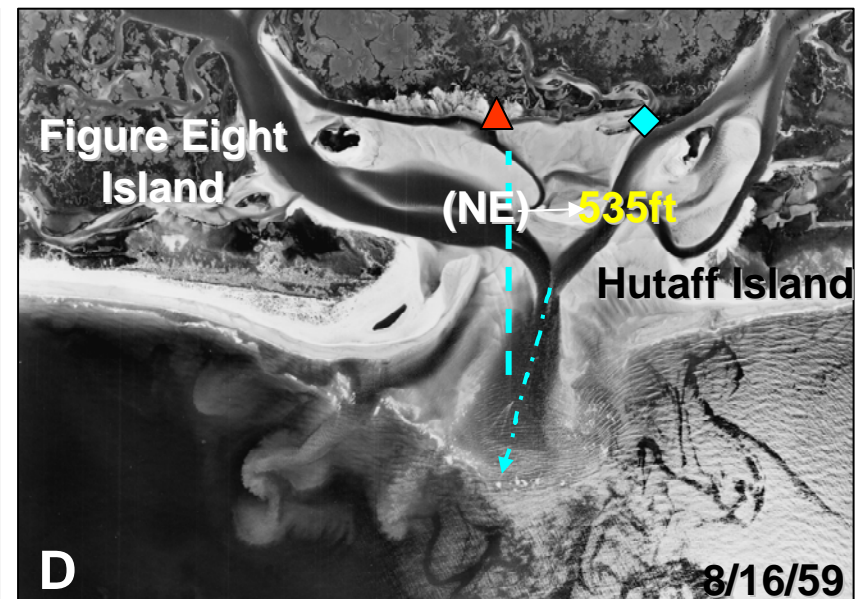
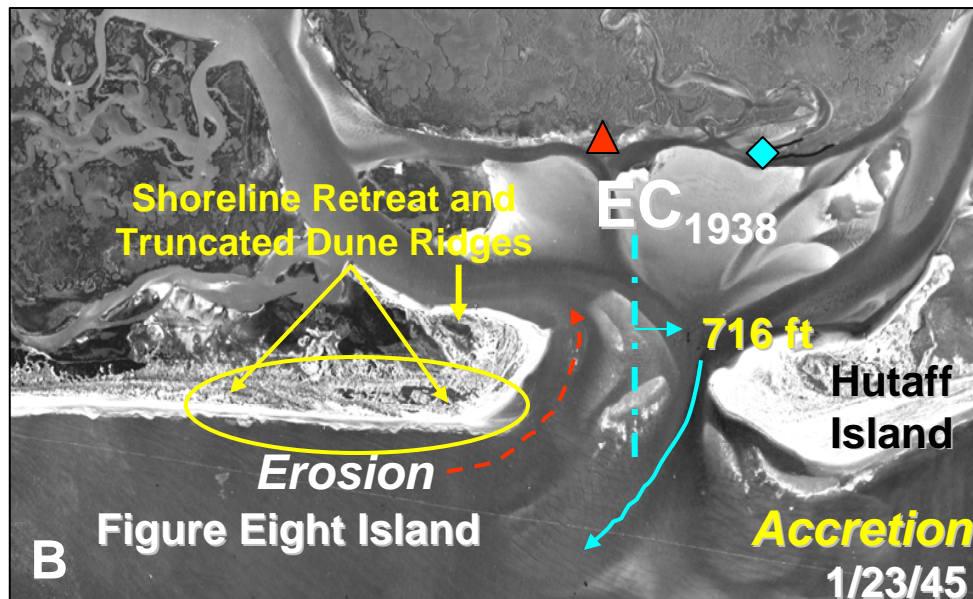
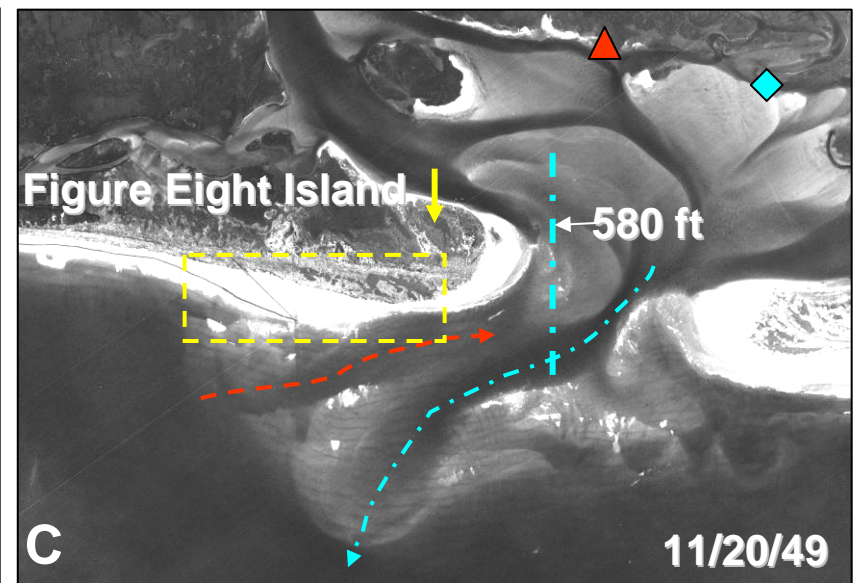


**Figure 16.** Historic aerial photographs (1938 – 1959) illustrating shoreline changes along F8I downdrift of Rich Inlet. **A.** View (5/17/38) of the north end of F8I showing accretion zone downdrift of Rich Inlet. **B.** View (1/23/45) of the erosion along the accretion zone. Note truncated dune ridges and the encroachment of the flood channel due to the skewed ebb channel. Also note the progradation of the HI shoreline. **C.** View (11/20/49) depicting the skewed ebb channel and the buildup of the shoreline in the lee of the flood channel. Note the erosion of the HI oceanfront. **D.** View (8/16/59) showing progradation of the F8I oceanfront and inlet margin accretion (spit buildup). The erosion of HI is due to the NE shift of the ebb channel and development of the flood channel. Red triangle and light blue diamond are reference points.



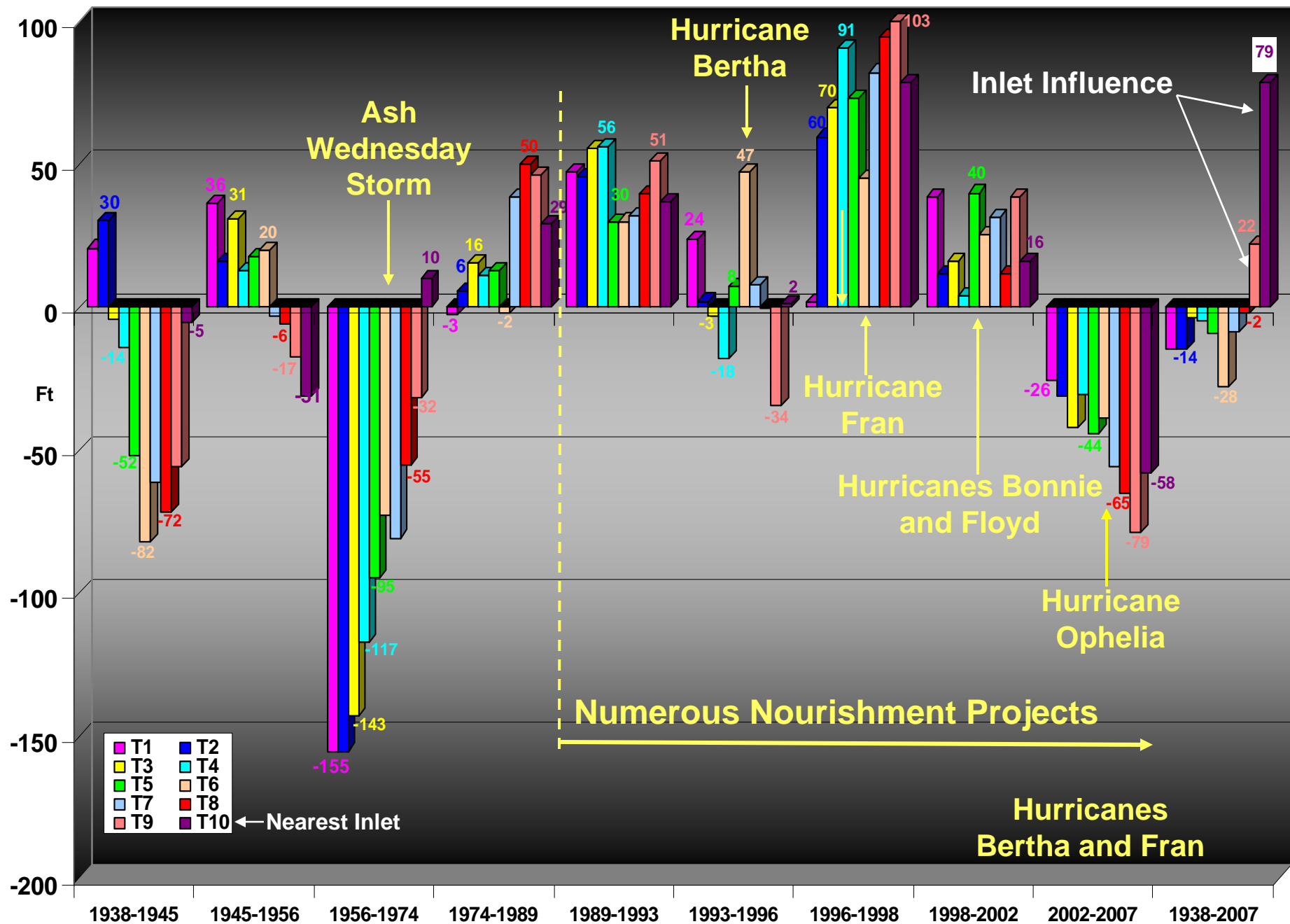


**Figure 17.** Bar graph depicting short-term shoreline changes from 1938 to 2007 along F8I between the T1 –T 10 the reach that lies outside the IHA.



**Figure 18.** Aerial photographs depicting condition of nourished oceanfront shoreline prior to mid 1984 erosion episode. **A.** and **B.** (5/20/84). Views of nourished shoreline segment and swash bar welding onto F8I. **C.** View (5/20/84) showing the onset of erosion of redeveloping inlet shoreline **D.** Landward view (5/20/89) of Rich Inlet showing spit development along scarp inlet shoreline. Note lack of shrub line along scarp line.



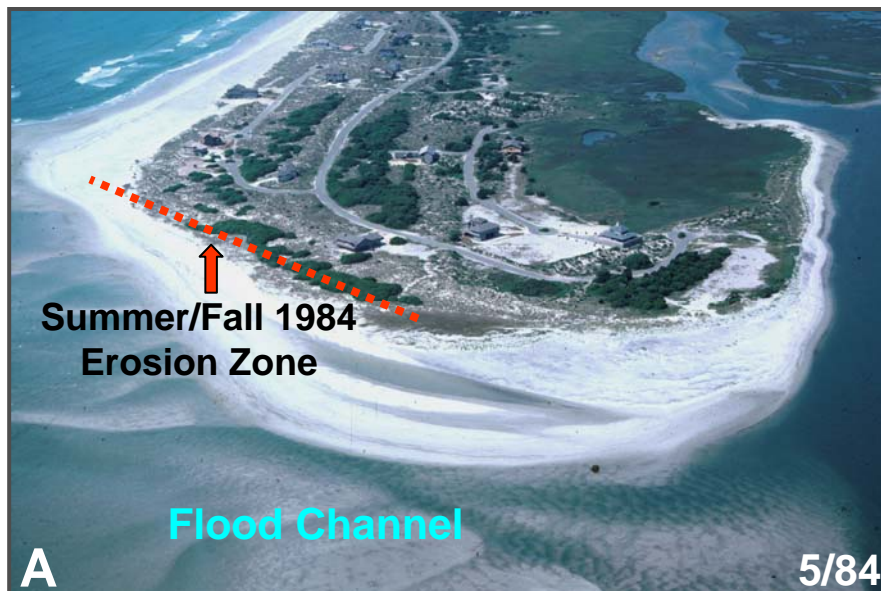


**Figure 19.** Oblique aerial photographs of F8I and Rich's Inlet shoreline during 1984. **A.** Seaward view of the inlet shoreline depicting the redeveloping spit, ridge and swale features, and the intact shrub line. **B.** Oblique aerial photograph depicting very rapid erosion of the inlet shoreline and dying shrub thickets. Compare to "A". **C.** Landward view (9/84) of eroded and scalloped inlet shoreline. **D.** Landward view (9/89) of rebuilt and elongating inlet shoreline spit. Note the occluded channel adjacent to the scarped uplands and the lack of shrubs. By 1993 the spit had enlarged considerably and the flood channel had infilled while the mid-inlet shoal became incorporated into the barrier.



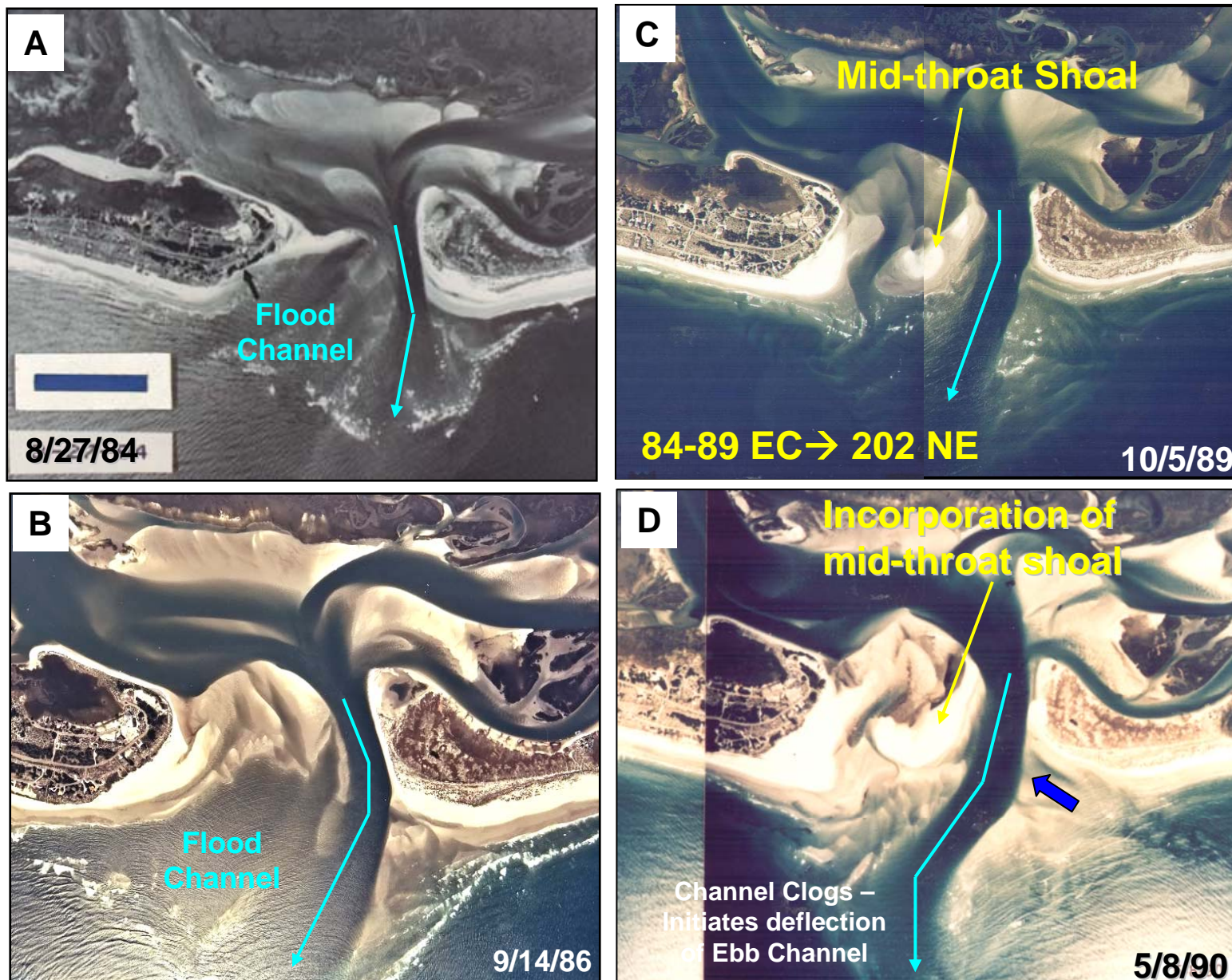


**Figure 20.** Aerial photographs (8/84- 5/90) of flood channel changes along F8I margin. **A.** View (8/27/84) of erosion along F8I shoreline. Note position of ebb channel. **B.** View (9/14/86) of redeveloped spit along F8I inlet margin. **C.** View ( 10/5/89) of mid throat shoal and northward developing spit. **D.** View (5/8/90) of nearly infilled flood channel. Note narrow inlet and initial incorporation of mid throat shoal



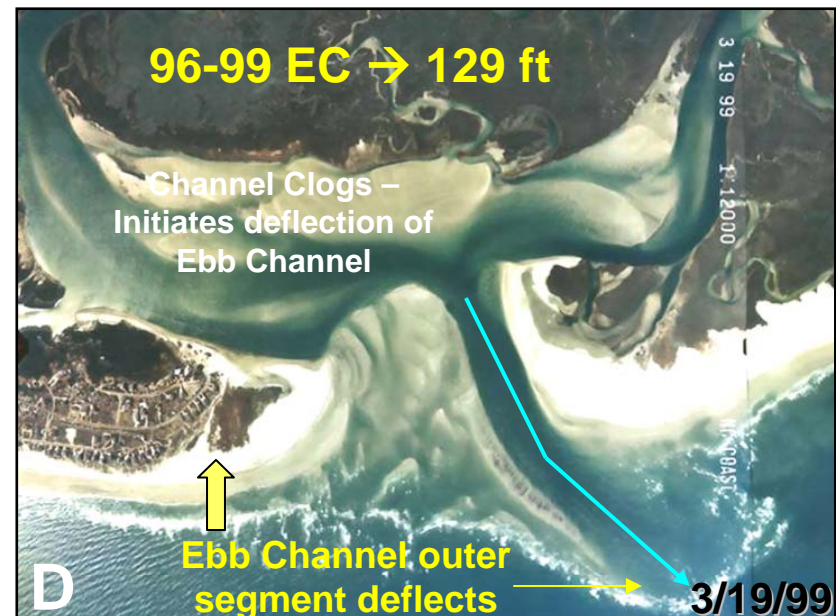
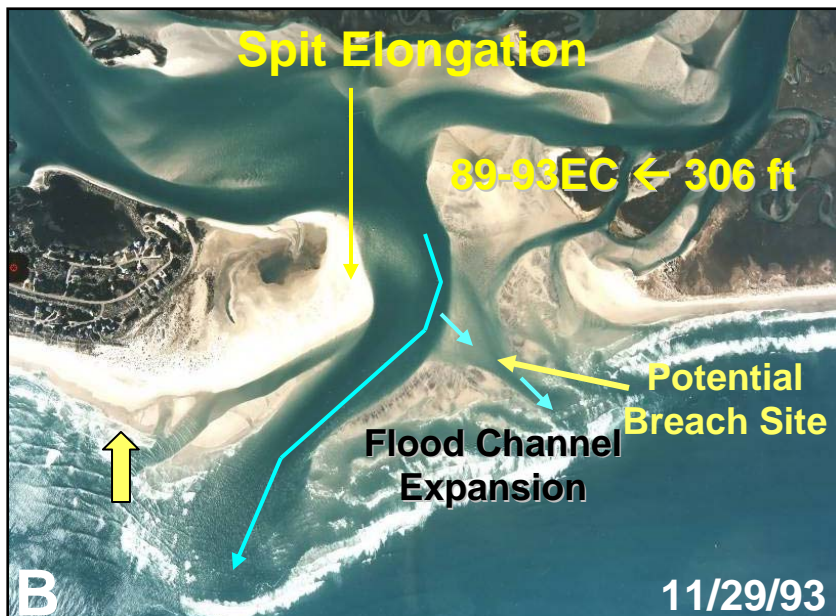
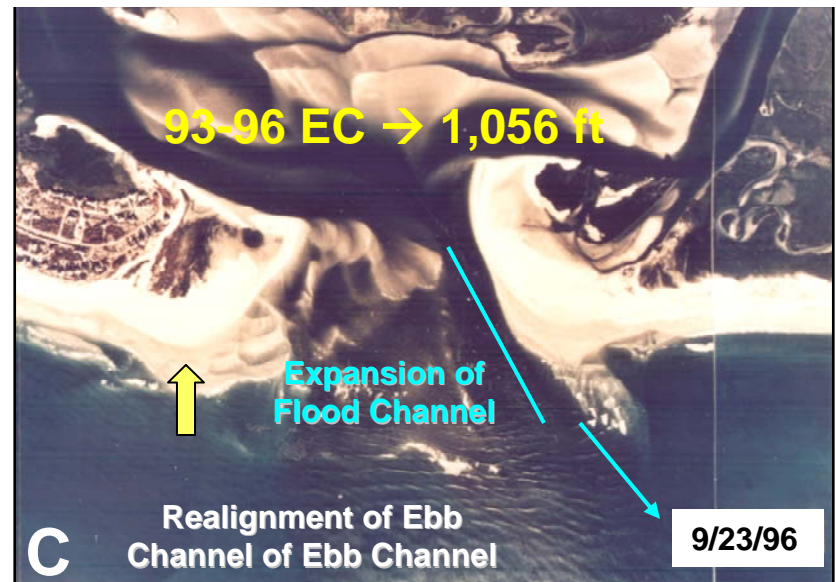
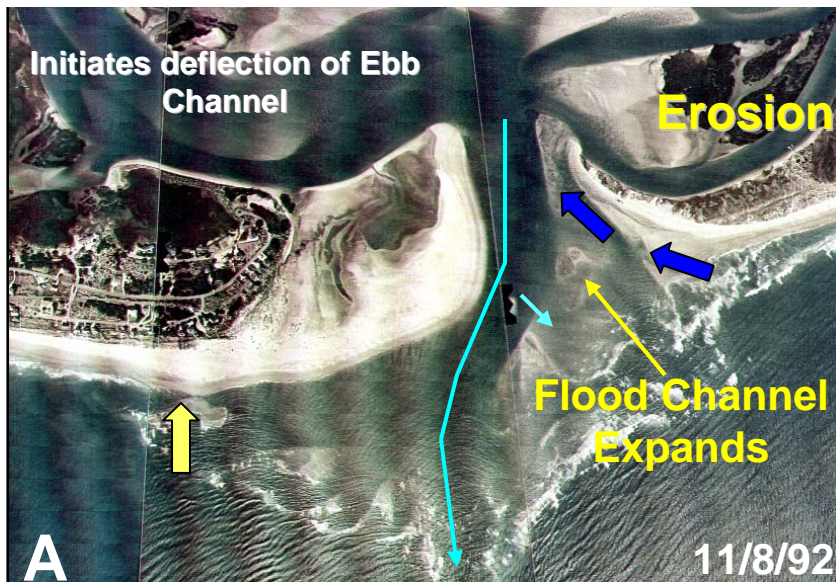


**Figure 21.** Aerial photographs of Rich Inlet (11/92-3/99). Photographs depict oceanfront shoreline changes related to ebb delta breaching and ebb channel deflection (A-D), spit development/erosion on F8I inlet margin and changes in the symmetry of the ebb-tidal delta (A-D). Note the change in the wave-sheltering effect with channel shift to NE (B-D).



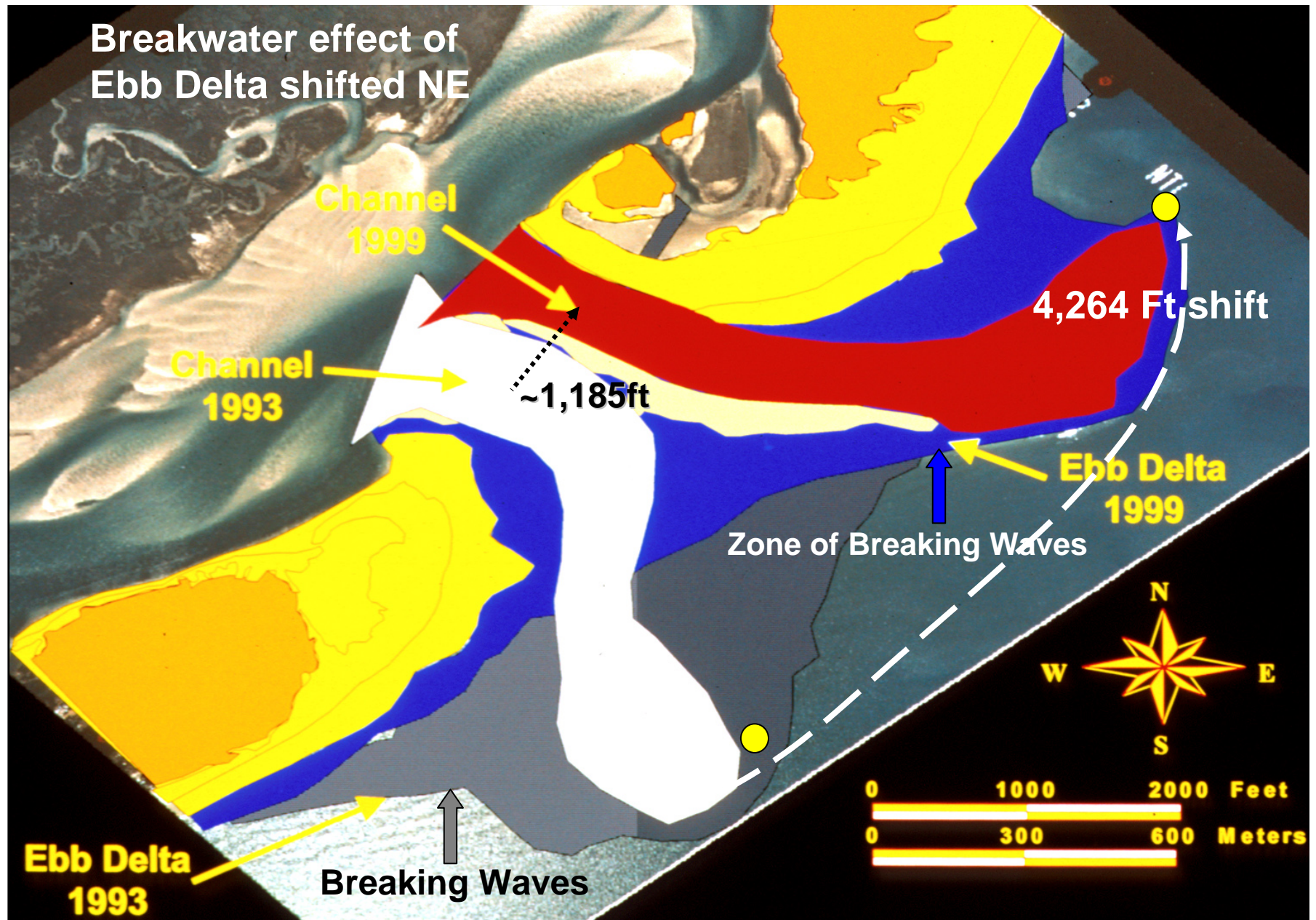


**Figure 22.** Cartoon illustrating the effects of ebb channel repositioning and outer channel realignment on the F8I oceanfront shoreline. The image shows the superposition of the 1993 and 1996 zone of breaking waves along the ebb-tidal delta and the location of the throat segment of the ebb channel. A NE shift of the ebb delta exposed the F8I oceanfront to incident waves. In this configuration swash bars no longer attached to the F8I oceanfront but rather moved into the flood channel and eventually the estuary and interior channels.



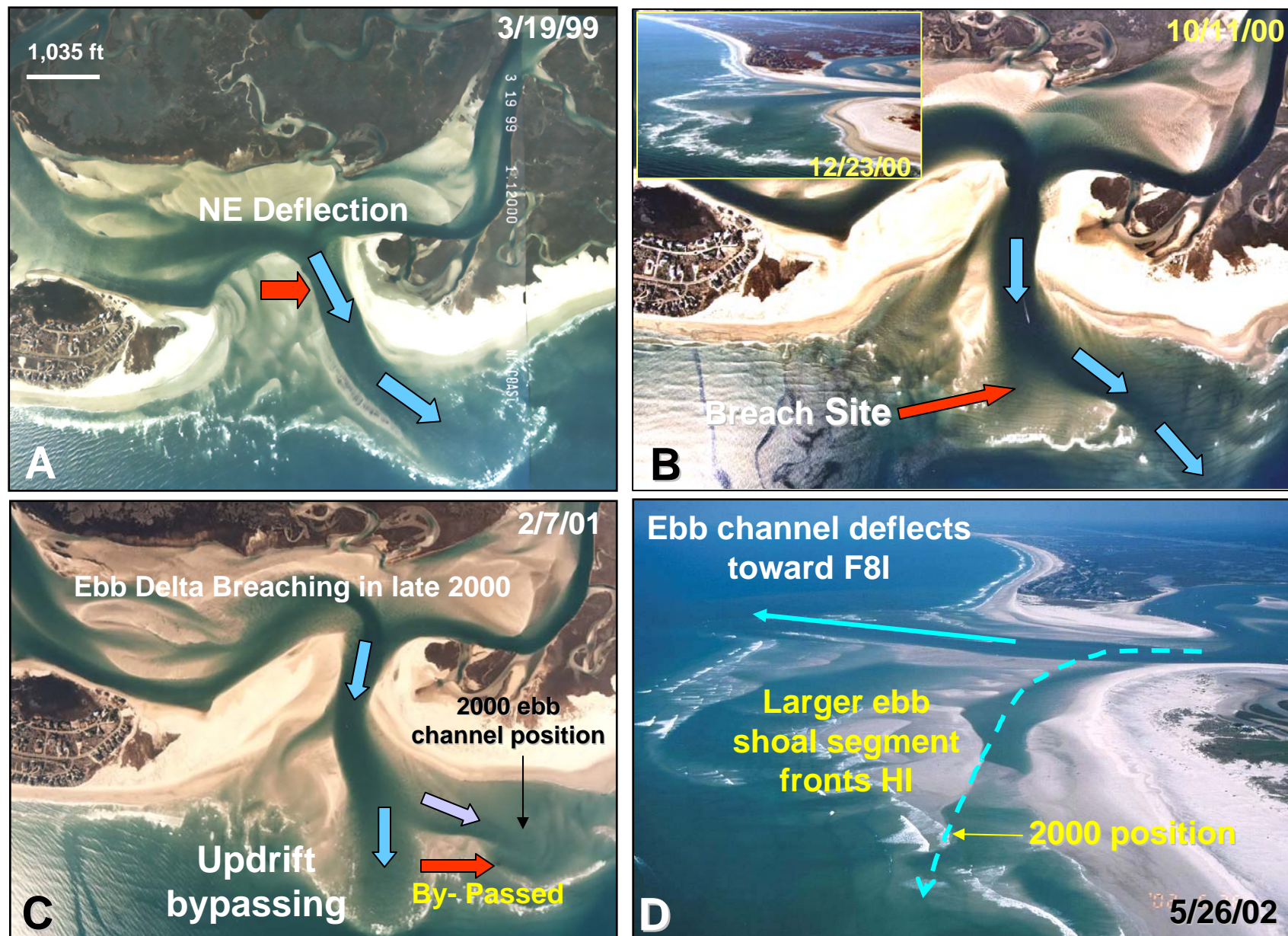


**Figure 23.** Aerial photographs (1999-2002) depicting the effects of ebb channel repositioning, realignment and bar by-passing. **A.** Image (3/19/99) depicts post-breaching deflection of ebb channel to NE. **B.** View (10/11/00) of ebb delta prior to beaching showing near breach. Insert shows breach. **C.** Photograph (2/7/01) depicts recent ebb delta breaching event (Dec 2000) and the large sand package in the process of being by-passed updrift. **D.** Southward view of ebb channel shifting southward and the larger ebb delta segment located NE of the channel fronting HI. Note the lack of any significant breakwater effect offshore F8I.



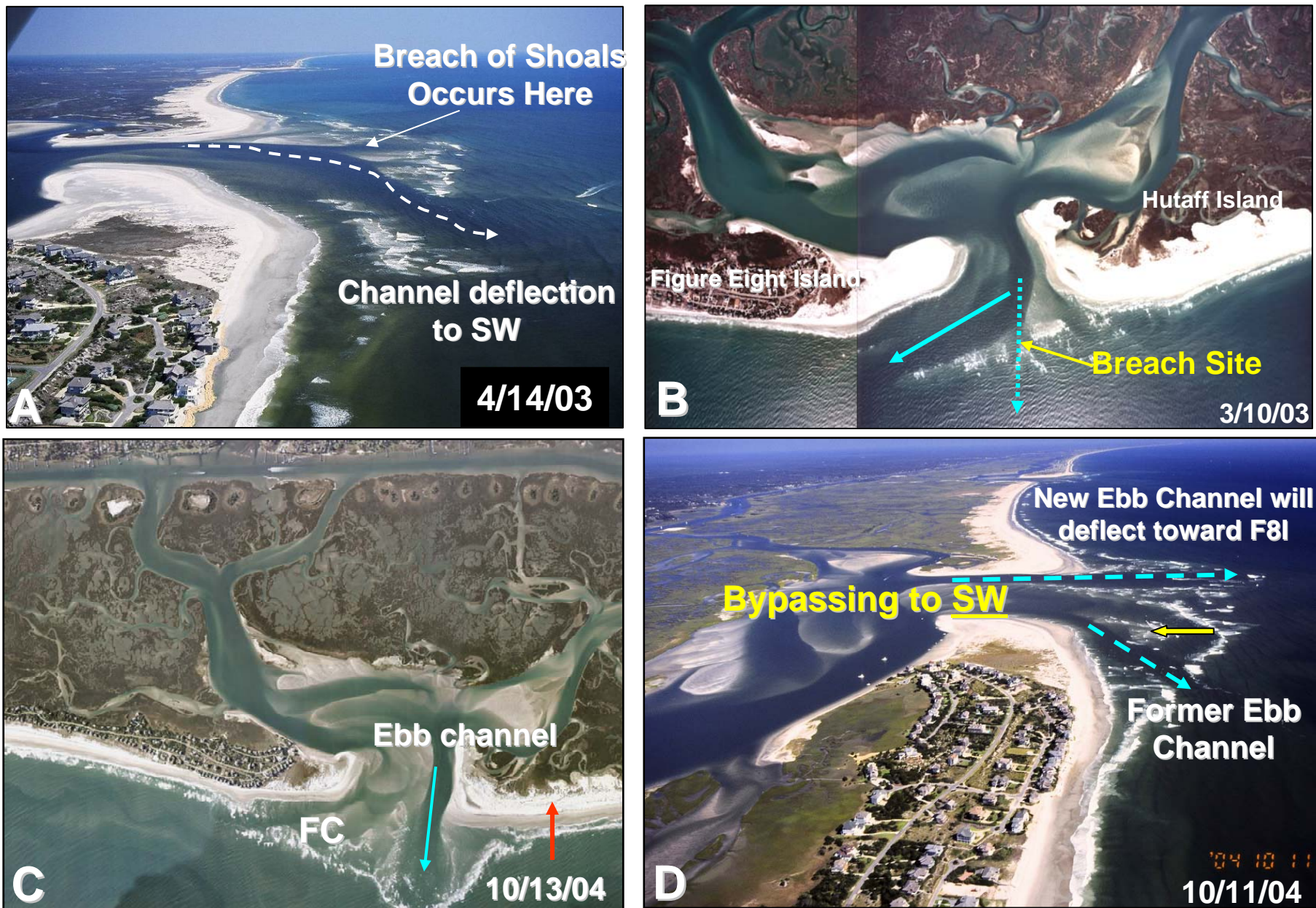


**Figure 24.** Aerial photographs (4/14/03- 10/11/04) depicting an ebb delta breaching event and SW bar by-passing event. **A.** Oblique image(4/14/03) showing channel aligned toward F8I. **B.** Photograph (3/10/03) depicting breach site note configuration of elongating spit. **C.** Image (10/13/04) illustrating realigned shore-normal ebb channel expanded flood channel adjacent to F8I. Note change in F8I spit. **D.** Oblique photograph depicting a NE view of former and new position of ebb channel. Ebb shoal segment depicted in “A and B” was by-passed to the SW.





**Figure 25.** Aerial photographs (A. 10/4/04, B. 4/5/05, C. 4/10/06 and D. 4/10/07) depicting recent shoreline and inlet changes. Note the alignment of the ebb channel has remained fairly constant since 2004 while the ebb channel has shifted ~ 415 ft toward F8I (SW) since 2004.



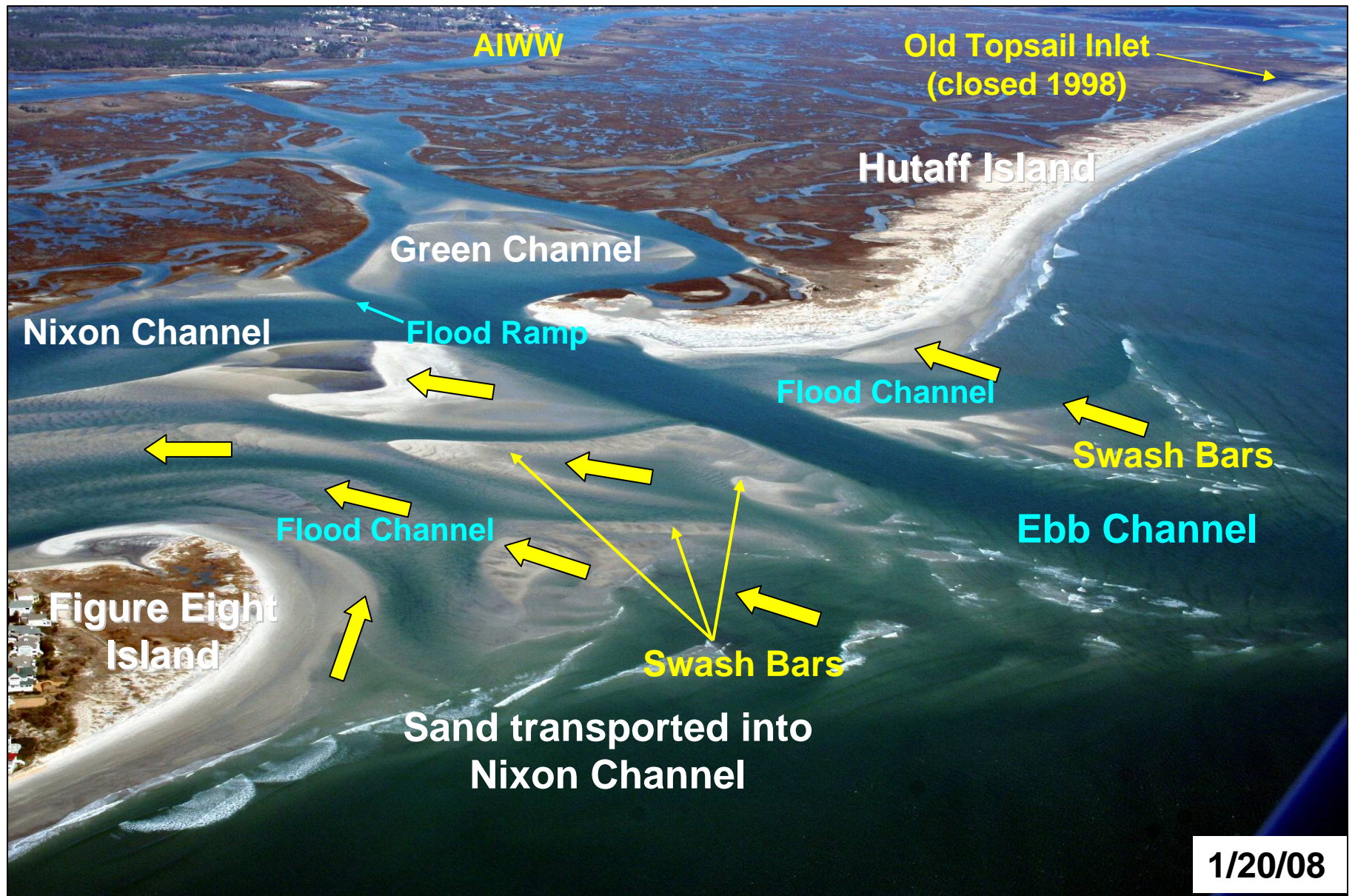


**Figure 26.** Oblique aerial photograph (1/20/08) of Rich Inlet and portions of the interior channels. Note the asymmetrically shaped ebb tidal delta and the location and alignment of the ebb channel. The wide marginal flood channel that abuts F8I is the major corridor for the transport of large volumes of sand into the estuary and Nixon Channel. Swash bars that formerly attached along F8I currently migrate through the flood channel. Note the attachment of swash bars along HI.



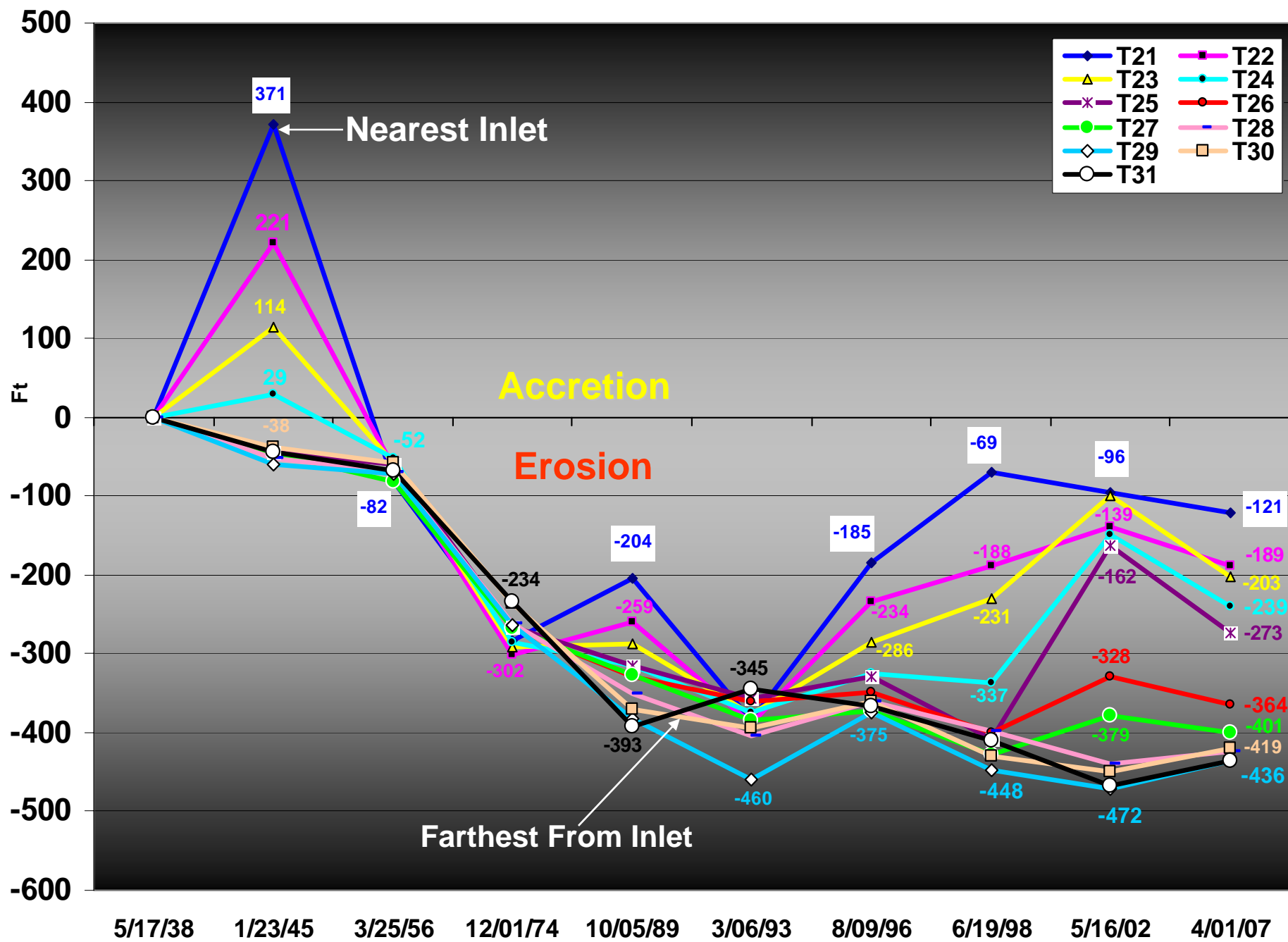


**Figure 27.** Graph depicting cumulative shoreline changes between 1938 and 2007 along transects T21 to T31 on HI. Note the shoreline at all transects has been characterized by net erosion that ranged from 121 to 436 ft. See Figure 13 for transect locations.

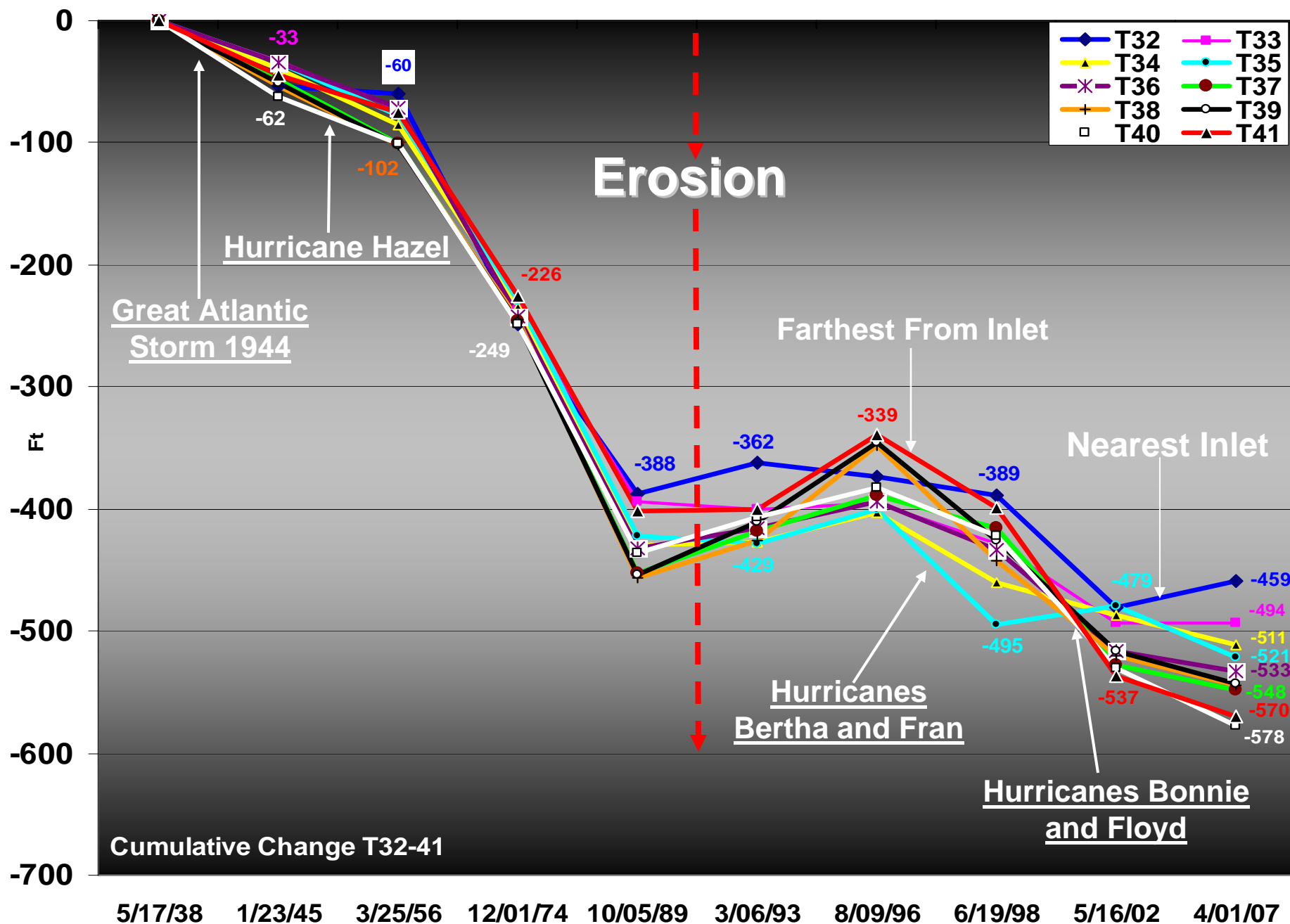


**Figure 28.** Graph depicting cumulative shoreline changes between 1938 and 2007 along transects T32 to T41 on HI. Note the shoreline at all transects has been characterized by net erosion that ranged from 459 to 578 ft. See Figure 13 for transect locations.



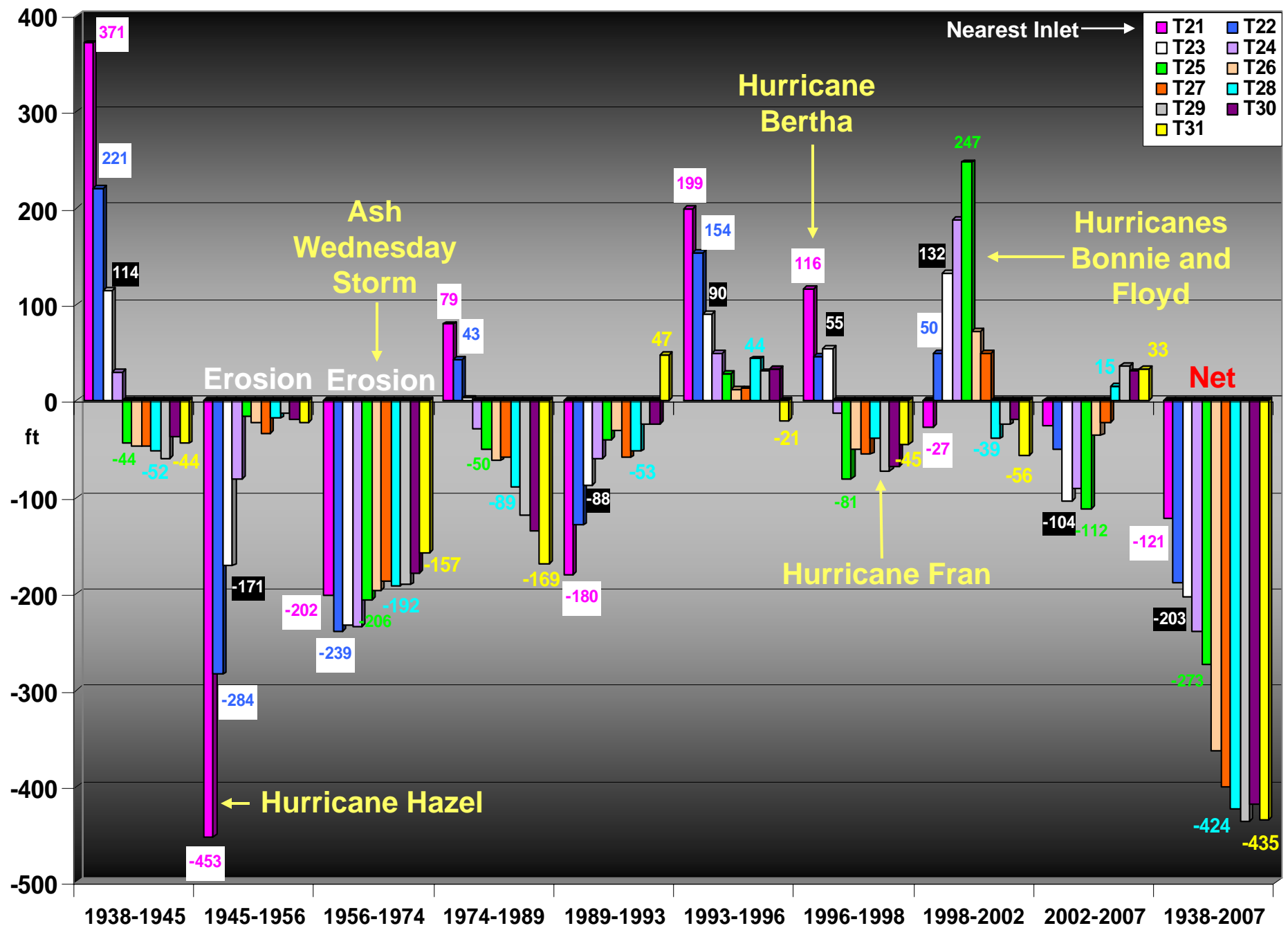


**Figure 29.** Bar graph depicting short-term shoreline changes along the HI oceanfront between the T21 and T 31 from 1938 to 2007. The entirety of the HI oceanfront shoreline lies within an IHA. Periods of accretion are inlet-related.

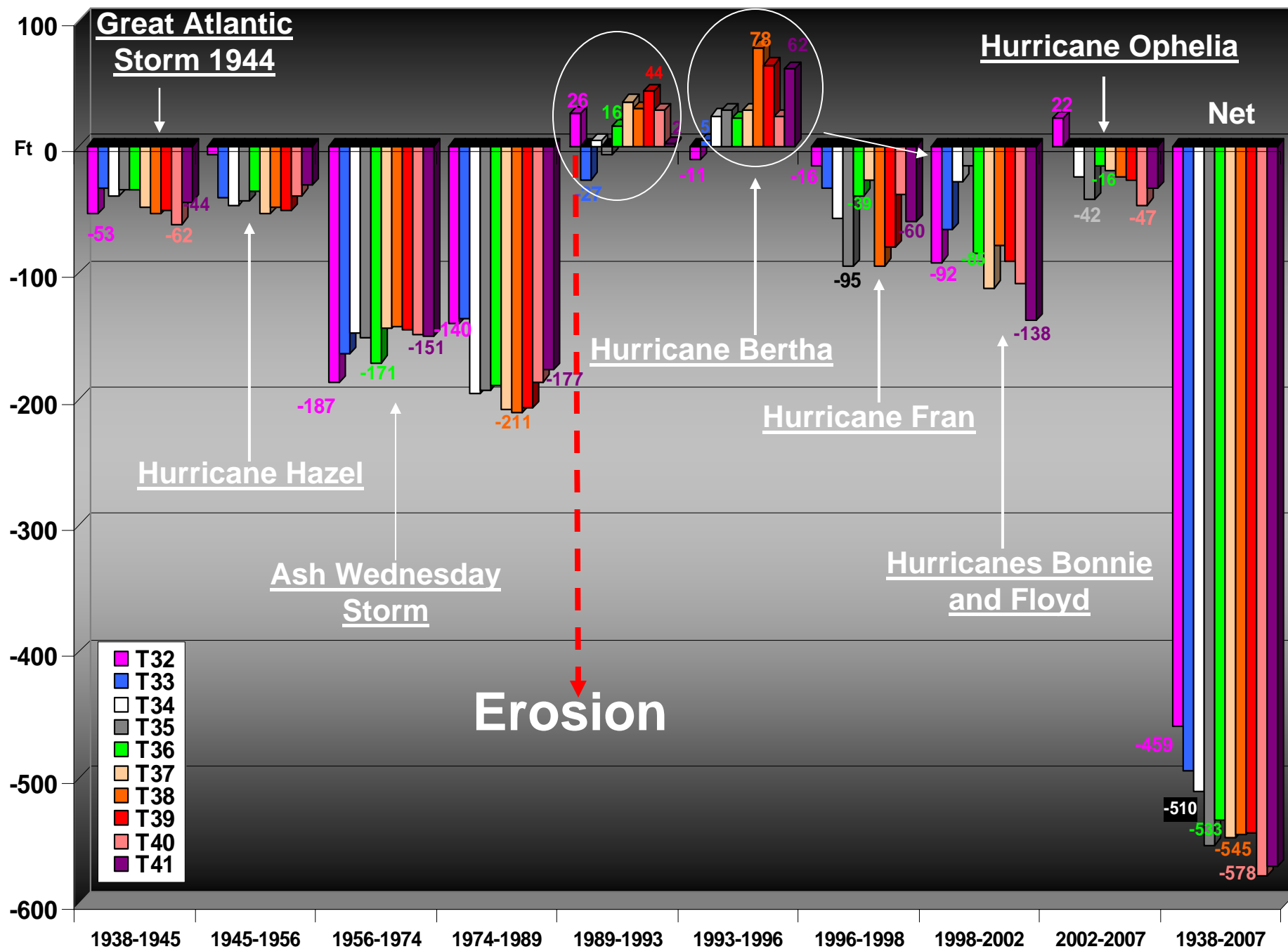
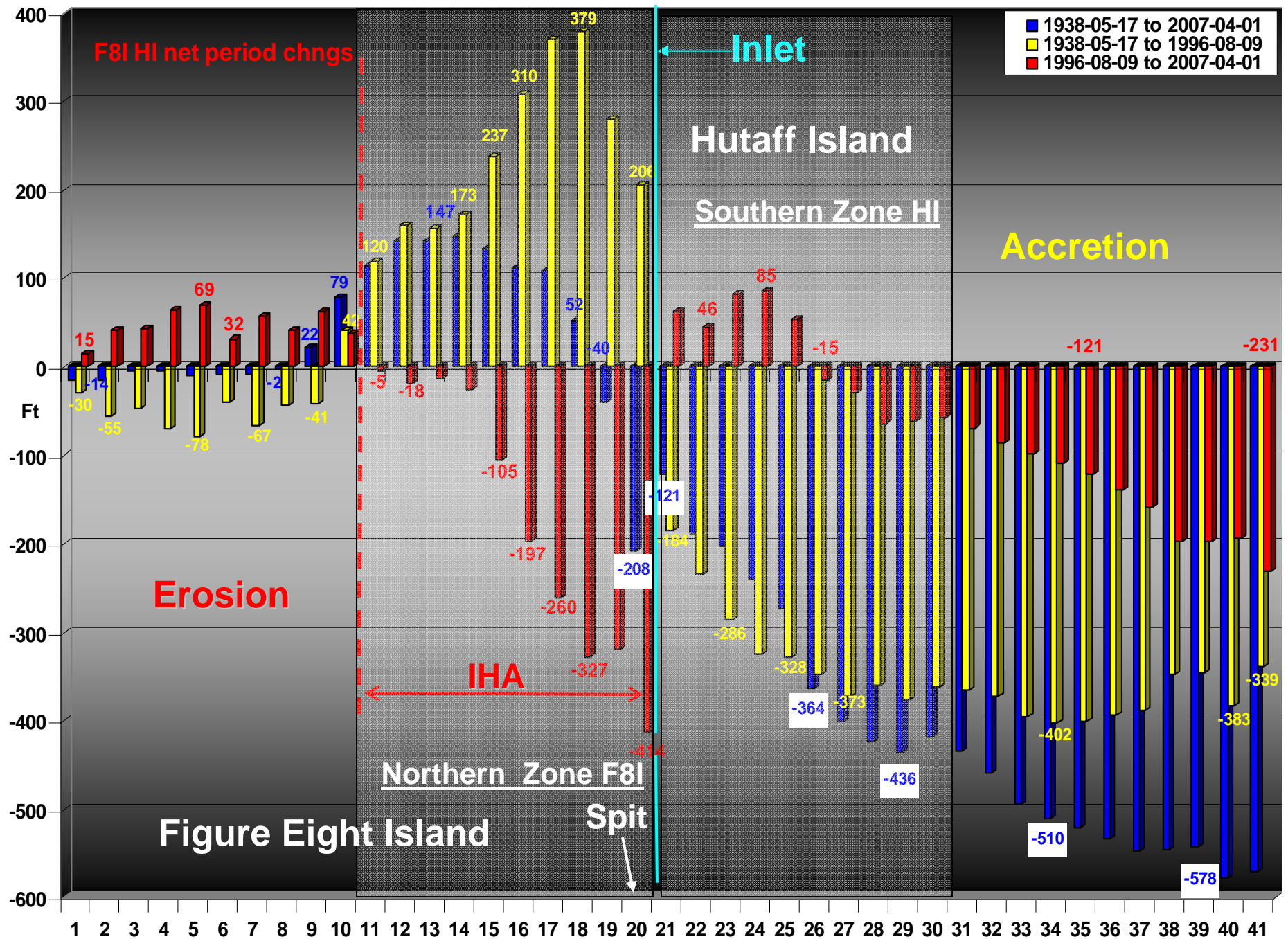
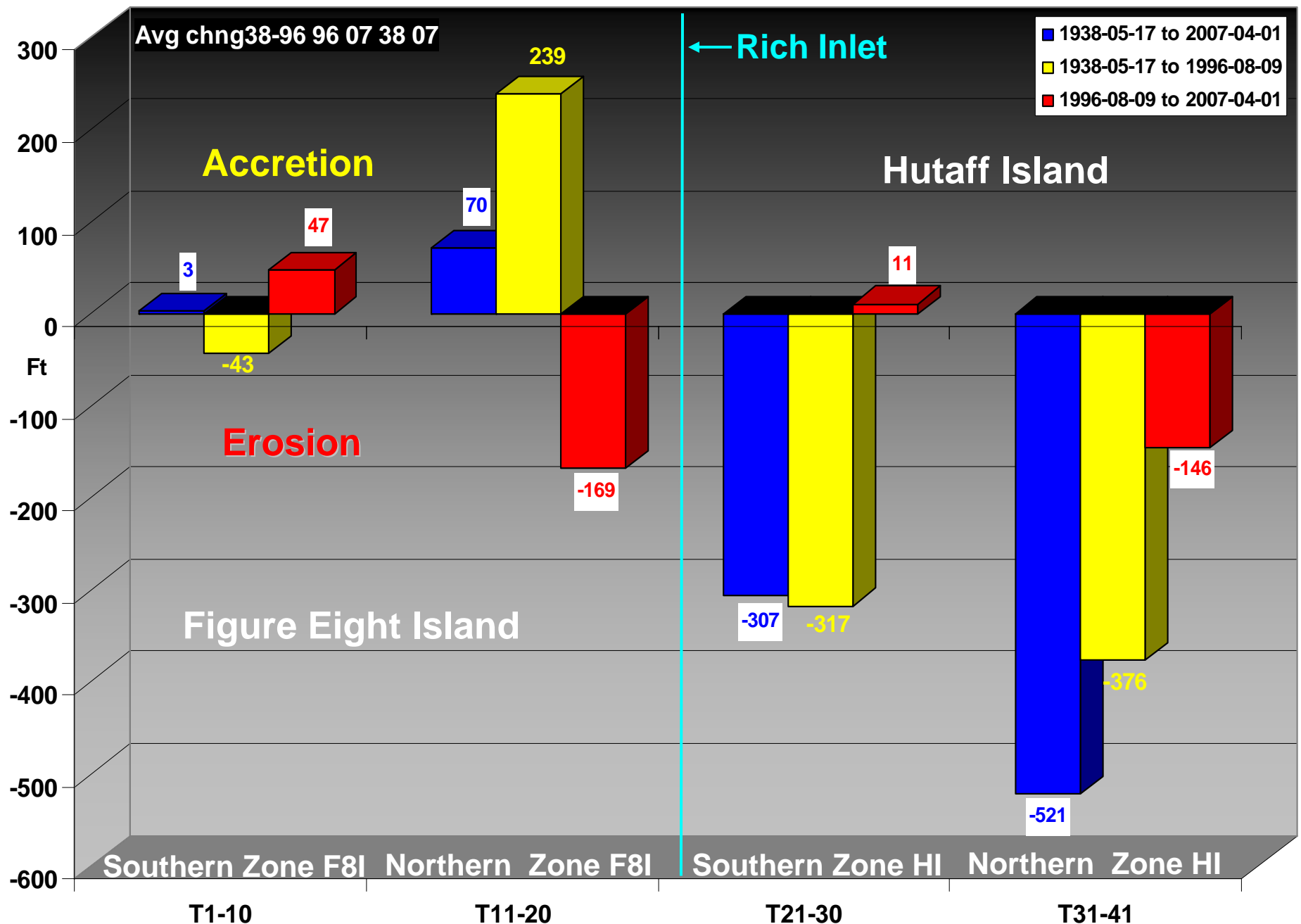


Figure 30. Bar graph depicting short-term shoreline changes along the HI oceanfront between the T32 and T 41 from 1938 to 2007.





**Figure 31.** Graph depicting the net shoreline changes along the F8I and HI oceanfront for selected periods of time between 1938 and 2007. A contrasting pattern of shoreline change characterizes F8I (Transects 1-20) and HI (Transects 21 - 41).



**Figure 32.** Graph depicting the average net shoreline changes along the F8I and HI oceanfront zones (T1-10, T11-20, T21-31 and T32-41) for selected periods of time between 1938 and 2007. A contrasting pattern of shoreline change characterizes F8I (Transects 1-20) and HI (Transects 21 - 41).



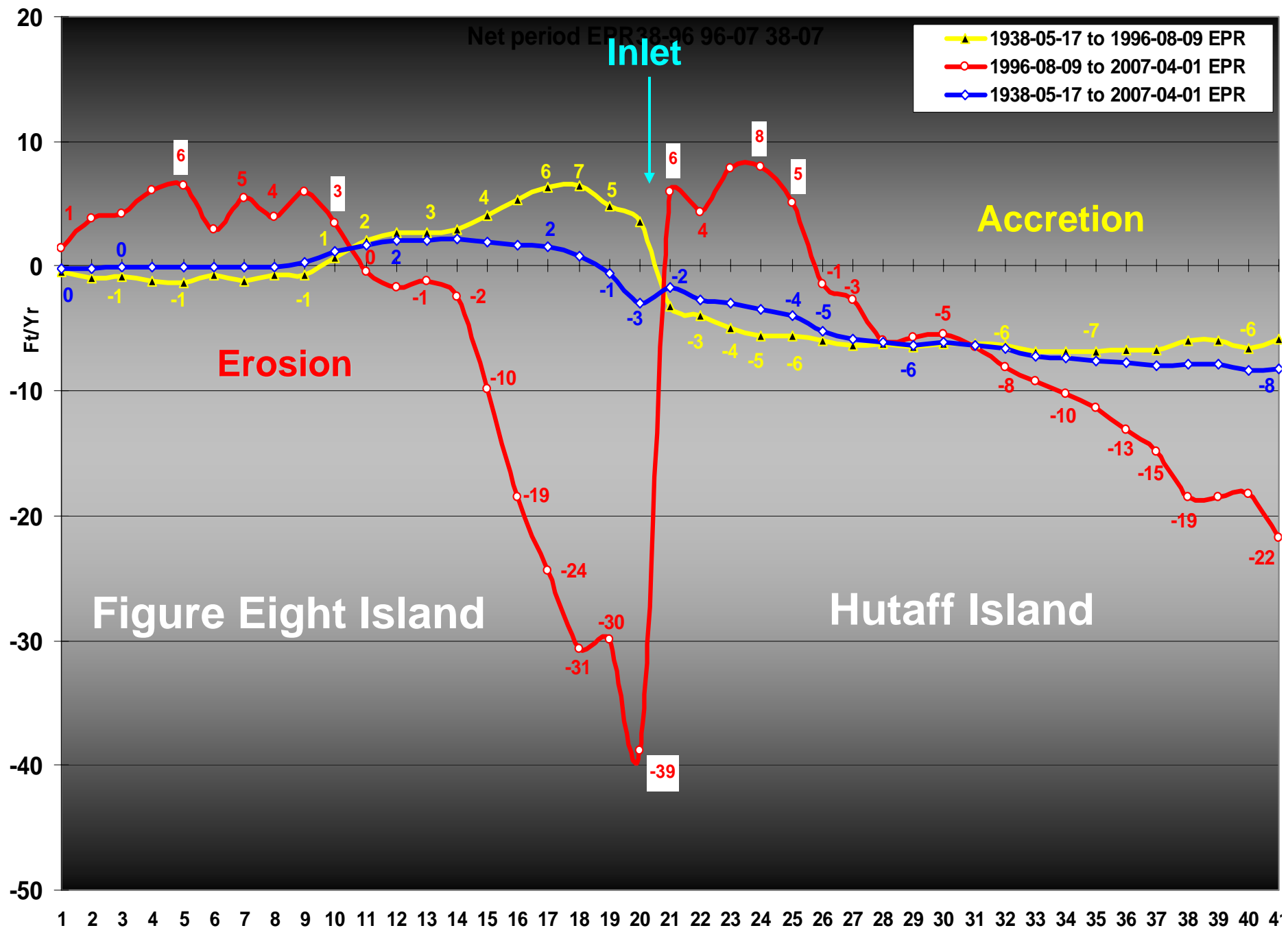


**Figure 33.** Graph depicting the shoreline change rates (end-point rate) for all transects along F8I and HI for various periods of time between 1938 and 2007.



**Figure 34.** Oblique aerial photograph (10/11/04) illustrating the oceanfront conditions along northern end of F8I, the interior channels and location of the estuarine erosion hot-spot (light blue dashed line box).



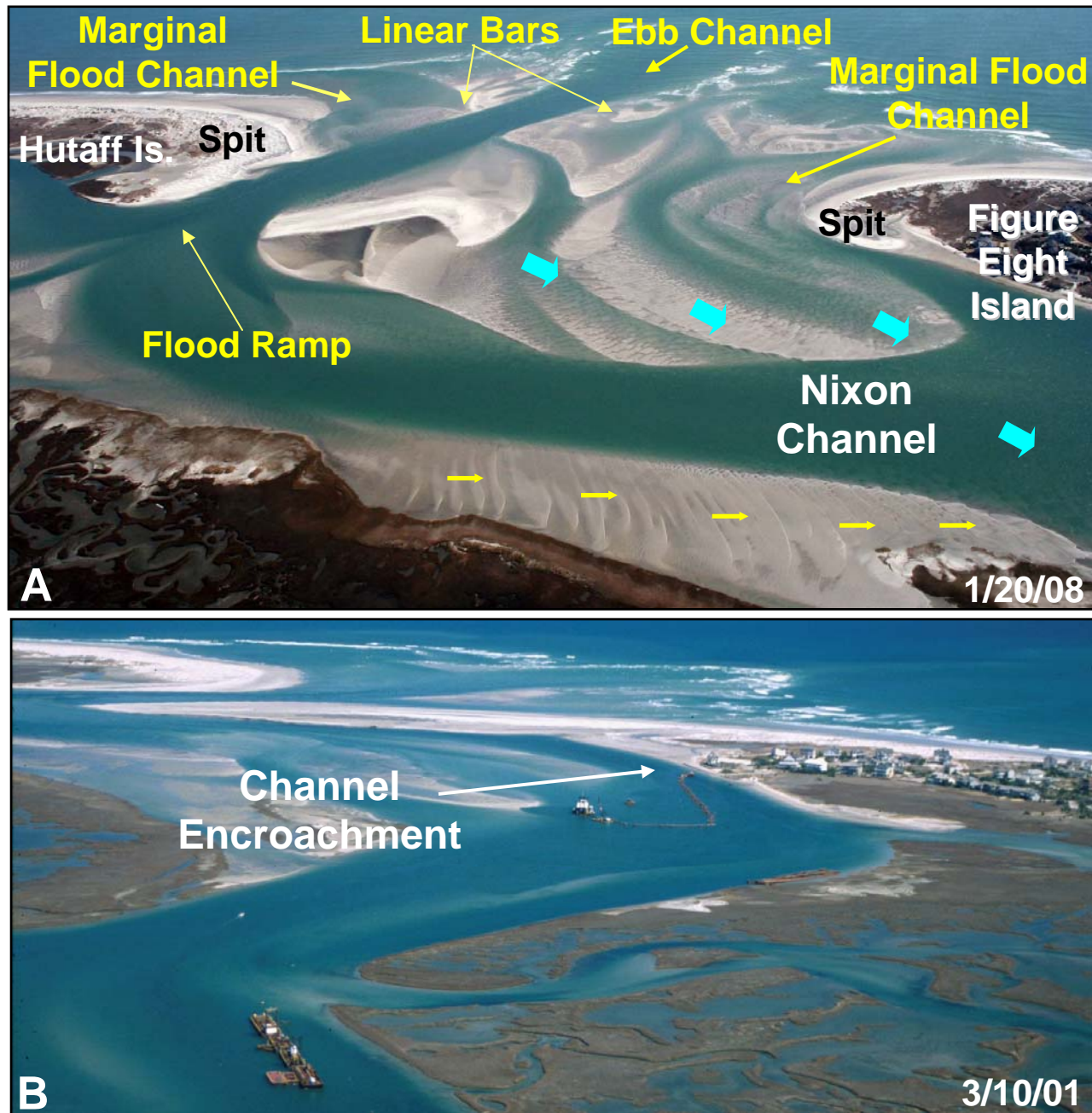


**Figure 35.** Aerial photographs depicting migration of bed forms (sand bars) and subsequent shoaling of the navigation channel. **A.** Seaward view (1/20/08) of the ebb and flood deltas and the multitude of bed forms. The majority of the sand packages are moving into Nixon Channel. **B.** Seaward view (3/10/01) of Nixon Channel depicting dredging operations associated with the 2001 nourishment project.



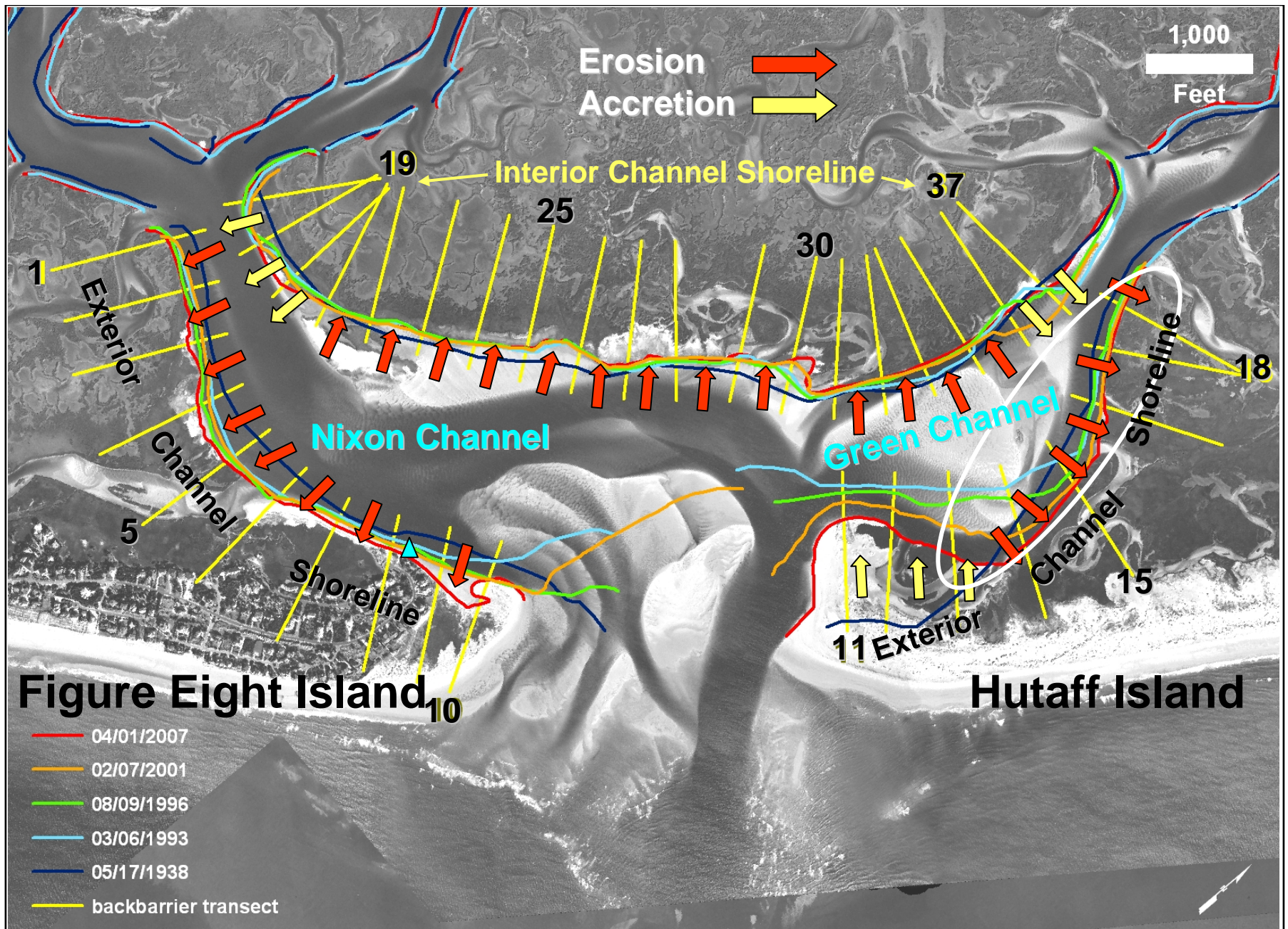


**Figure 36.** Aerial photograph (2007) depicting the location of transects along the margins of Green and Nixon Channels and the positions of the estuarine channel margins (selected years 1938-2007). Red colored arrows denote erosion while yellow arrows denote accretion.



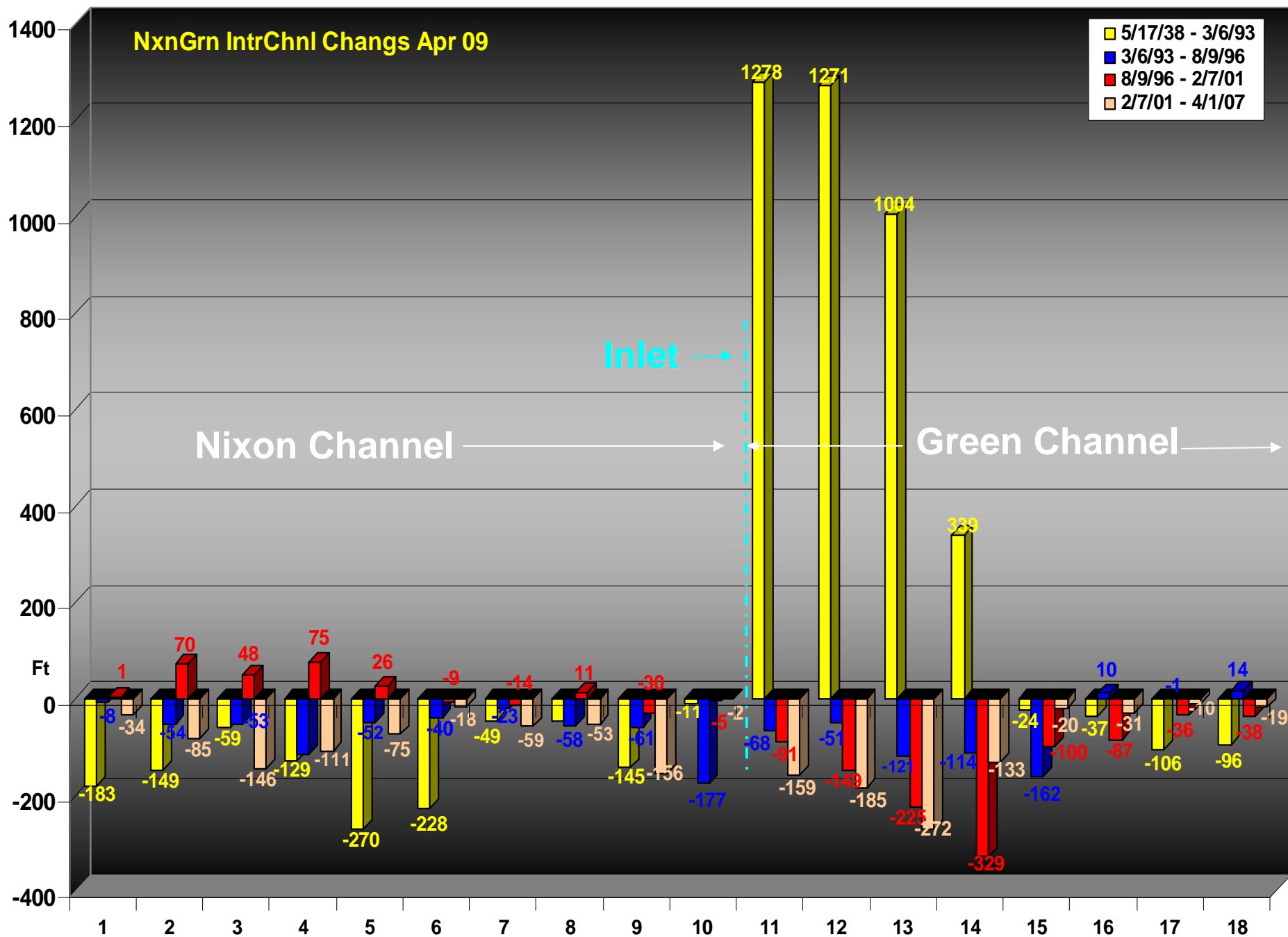


**Figure 37.** Bar graph illustrating net shoreline changes for various periods between 1938 and 2007 along the external (seaward) channel margin from T1 to T18. See Figure 36 for transect locations.

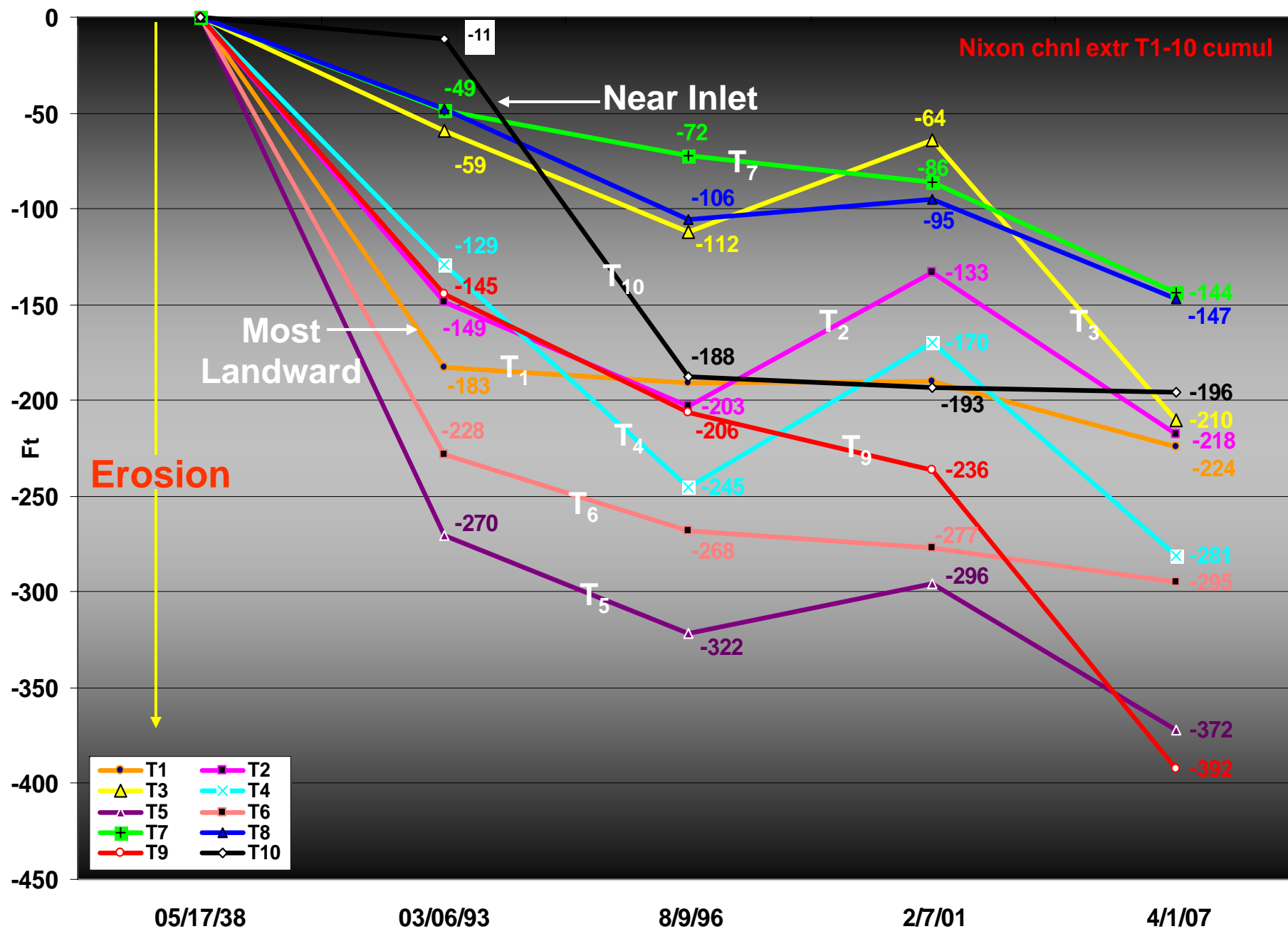


**Figure 38.** Graph depicting the cumulative shoreline change along the Nixon Channel exterior (seaward) margin. Note X axis is not to scale. See Figure 36 for location of transects along F8I channel margin.



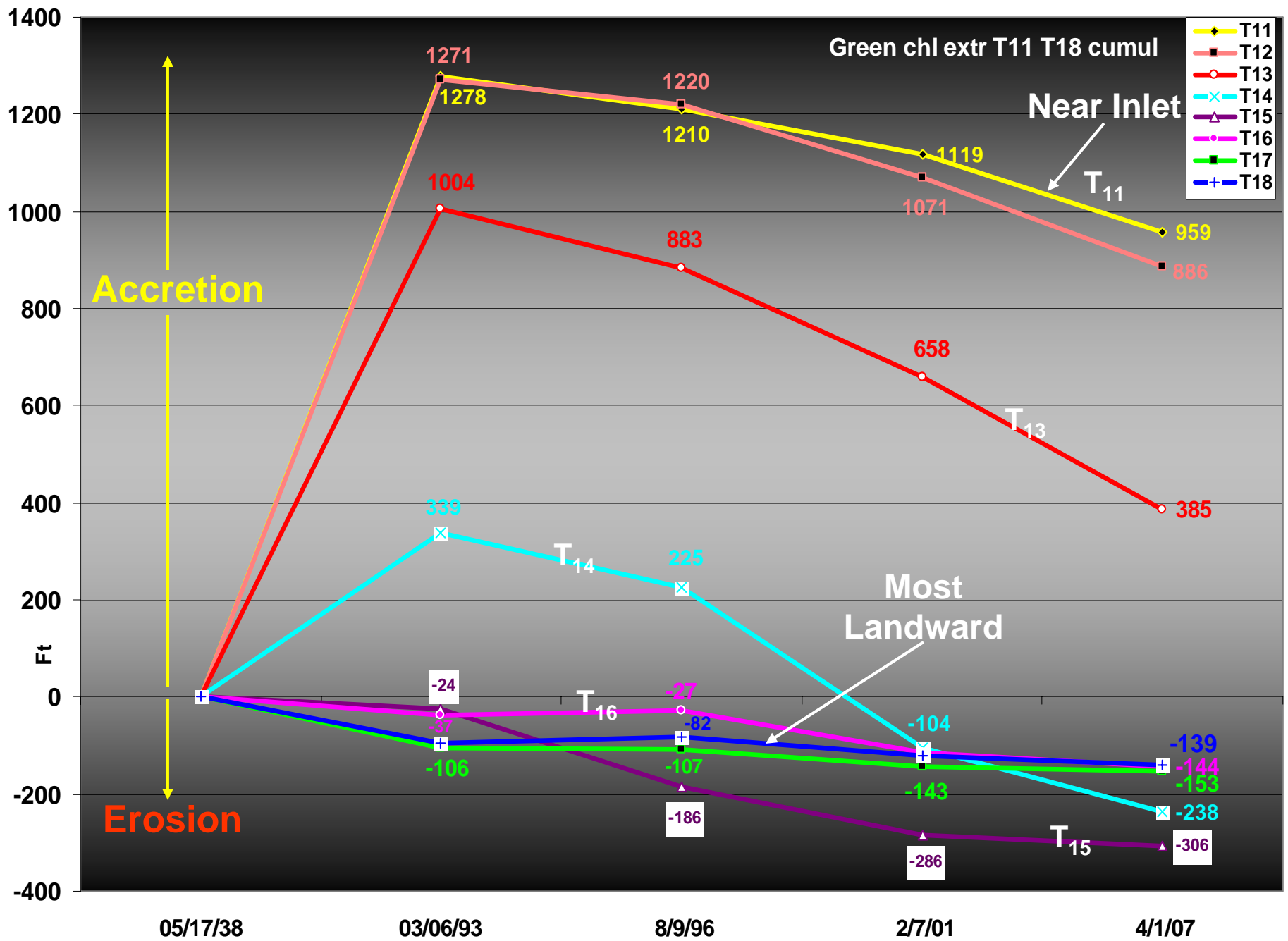


**Figure 39.** Graph depicting the cumulative shoreline change along the Green Channel exterior (seaward) margin. Note X axis is not to scale. See Figure 36 for location of transects along HI channel margin.

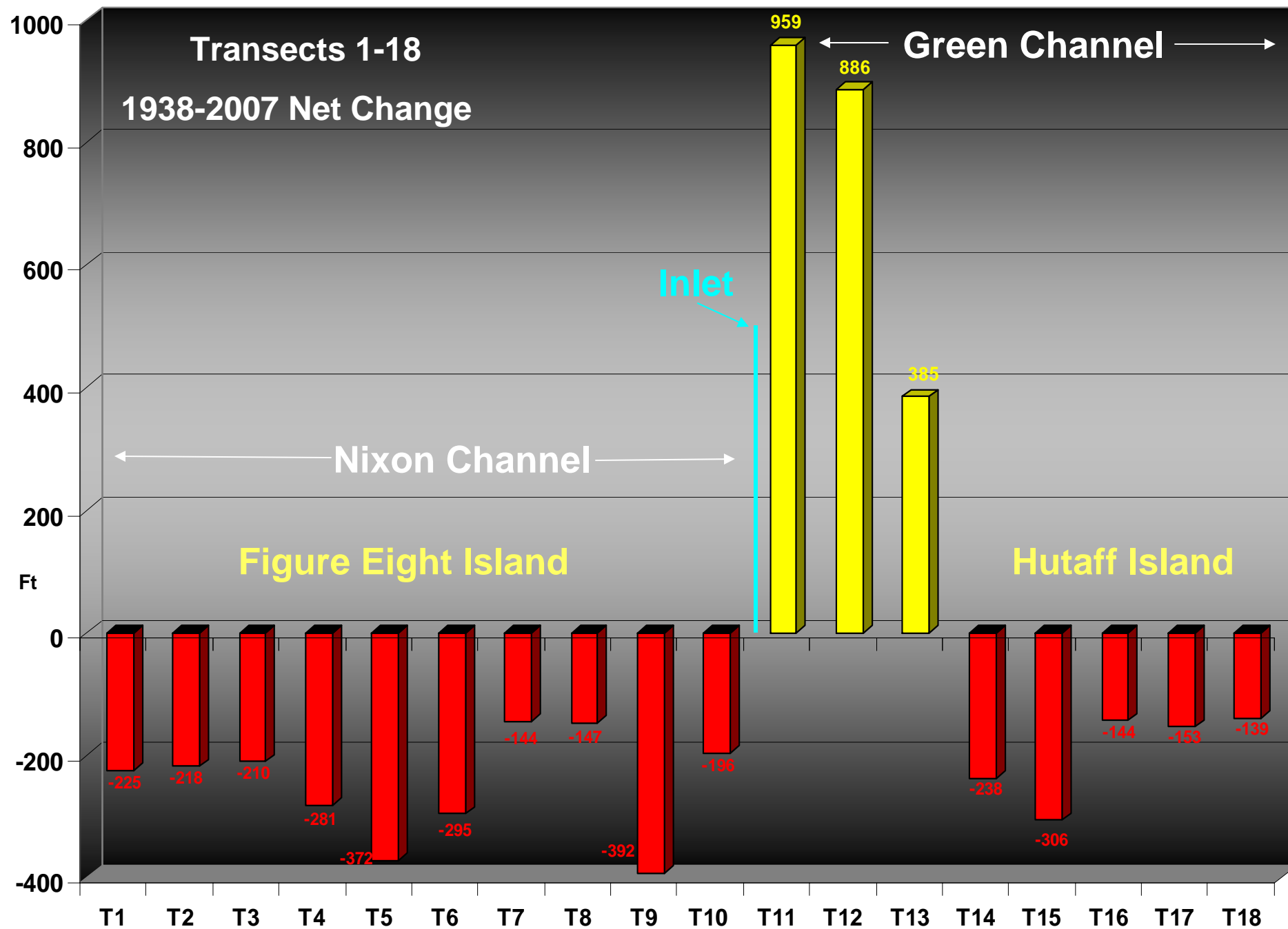


**Figure 40.** Bar graph depicting net shoreline change along external (seaward) margin (T1-T18) of Green and Nixon Channels from 1938-2007.



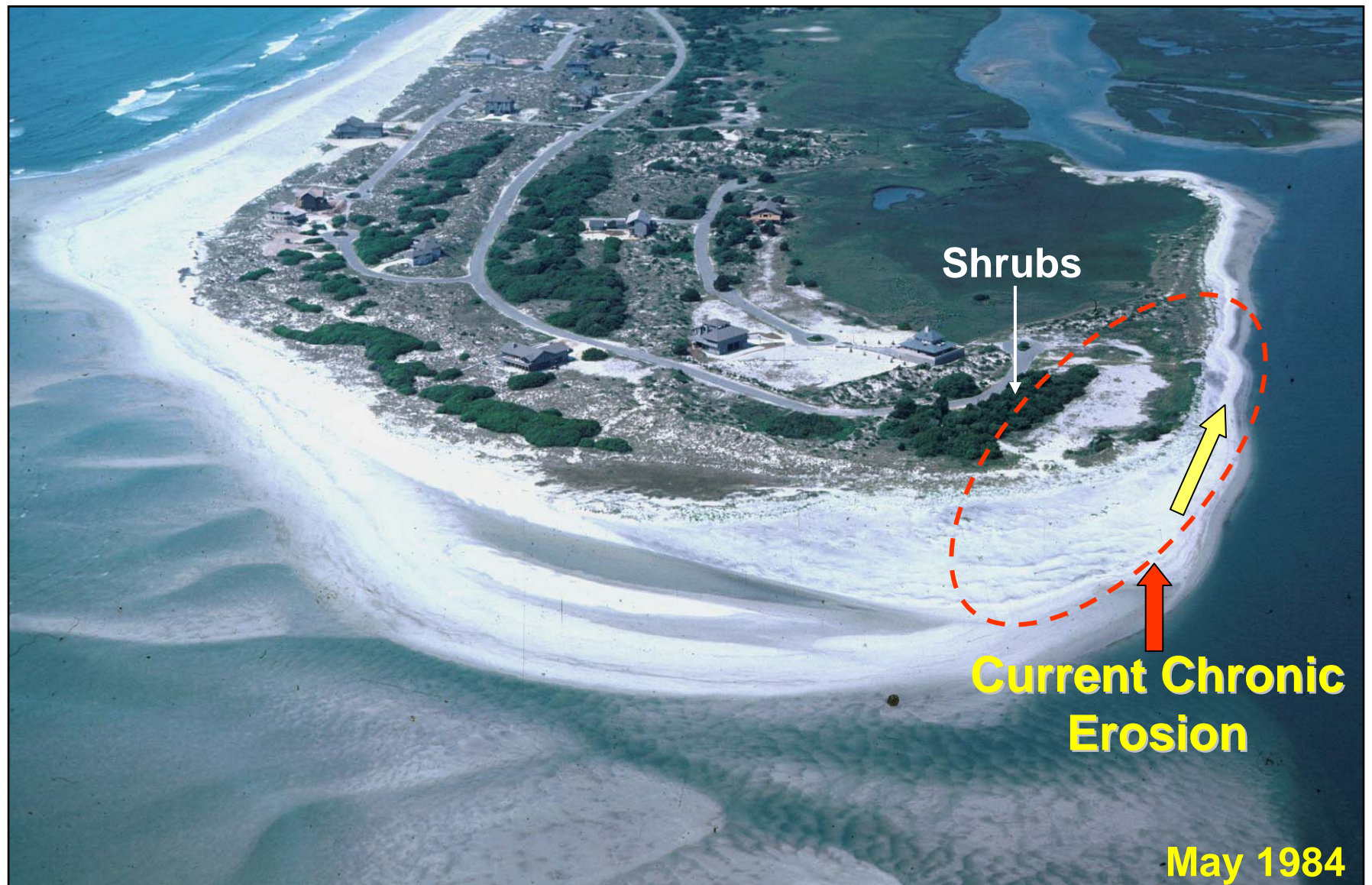


**Figure 41.** Oblique photograph (5/84) of the current erosion hot-spot along Nixon Channel. Note the relatively wide estuarine beach, dune field and shrubs. Also note the incipient spit development (yellow arrow).





**Figure 42.** Photographs depicting erosion and shoreline retreat along Nixon Channel shoreline between 9/99 and 2/08. **A.** Seaward view (9/99) of eroding channel margin shoreline. Thin veneer of sand mantles offshore peat subcrop. **B.** Seaward view (11/02) of peat exposure and shrub stumps. **C.** Seaward view (10/06) of peat exposure and sand accumulation due to wave swash. **D.** Seaward view (2/08) of newly emplaced sand bags.



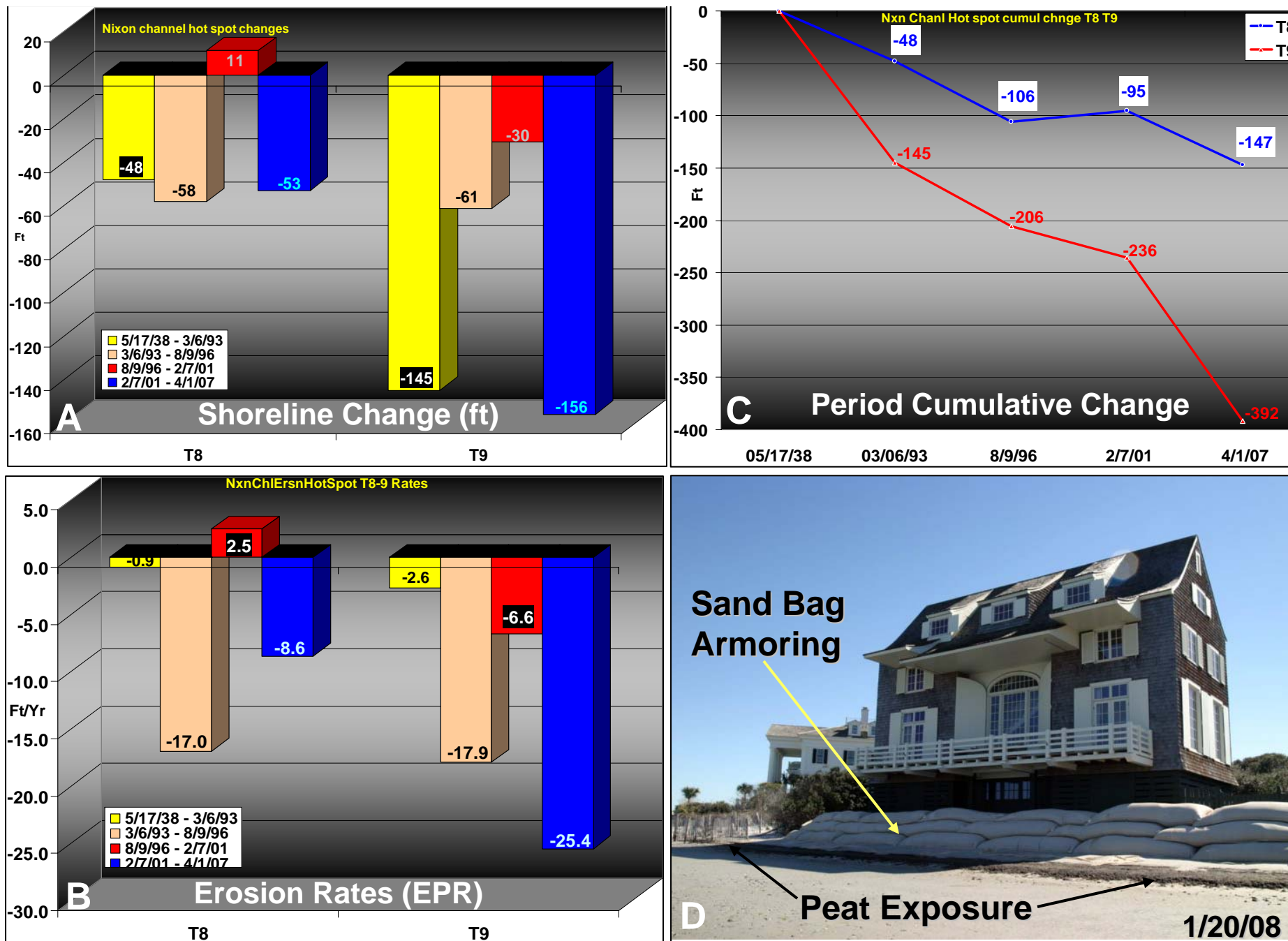


**Figure 43.** Estuarine channel erosion hot-spot (T8-9) along Nixon Channel. **A.** Shoreline graph for various periods between 1938-2007. **B.** Graph depicting T8-9 erosion rates (EPR). **C.** Graph of cumulative shoreline changes. **D.** Photograph (1/20/08) depicting armored shoreline and extensive peat exposure along low tide beach.



**Figure 44.** Photographs depicting erosion along a portion of the Nixon Channel shoreline. **A.** Landward view (5/3/07) illustrating erosion of the upland area. **B.** Landward view (5/3/07) of peat exposure along intertidal beach, stranded walkover and slumping of “sod”. **C.** Seaward view (2/19/08) of retreating shoreline imaged in “A” and “B”. **D.** Landward view (2/19/08) of structure in “A” and “C” and small scarp (red arrow) that extends toward adjacent home that is fronted by sand bags and a peat exposure.



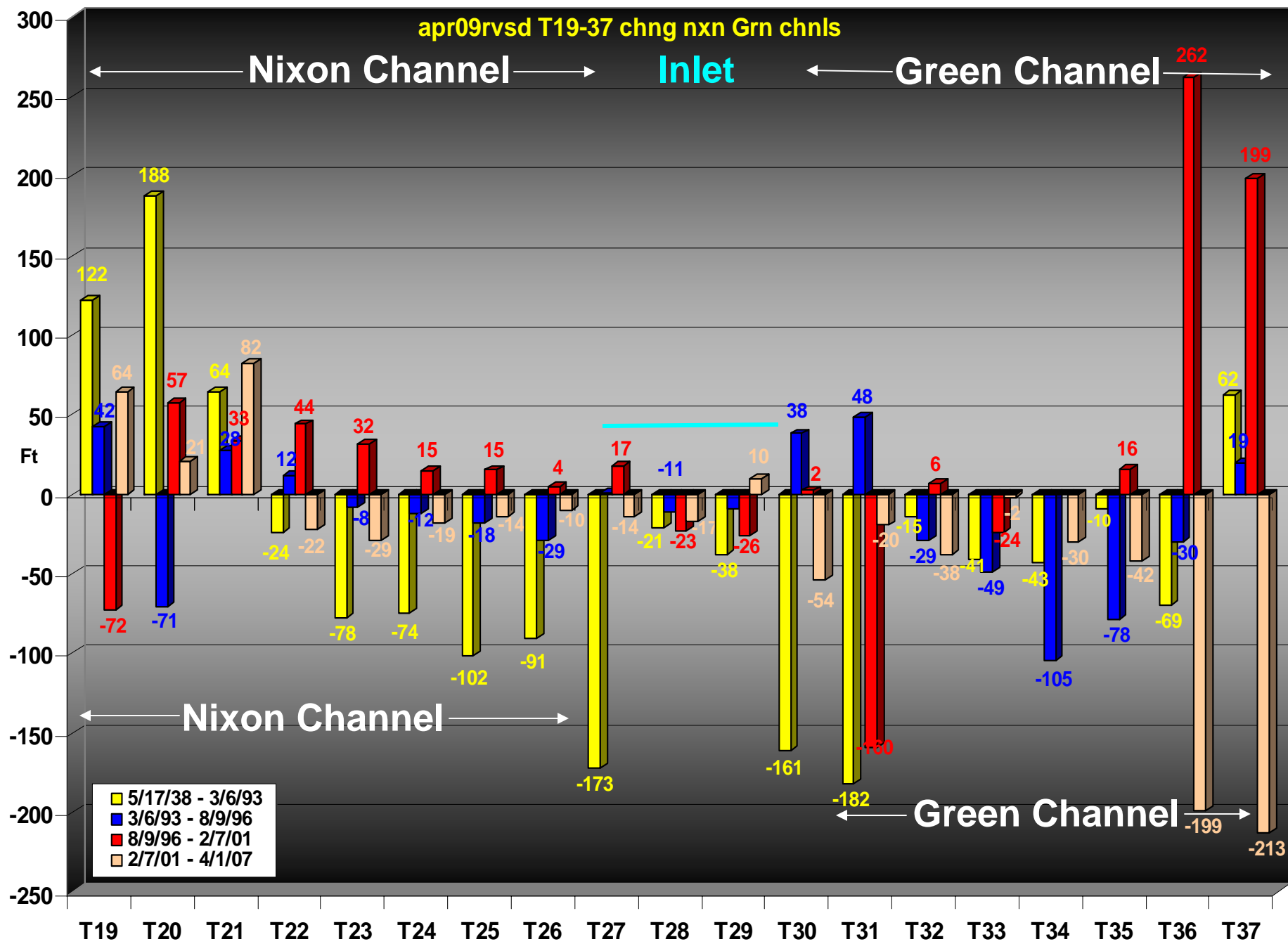


**Figure 45.** Bar graph illustrating net shoreline changes for various periods between 1938 and 2007 along the internal (landward) channel margin from T19 to T37. See Figure 36 for transect locations.

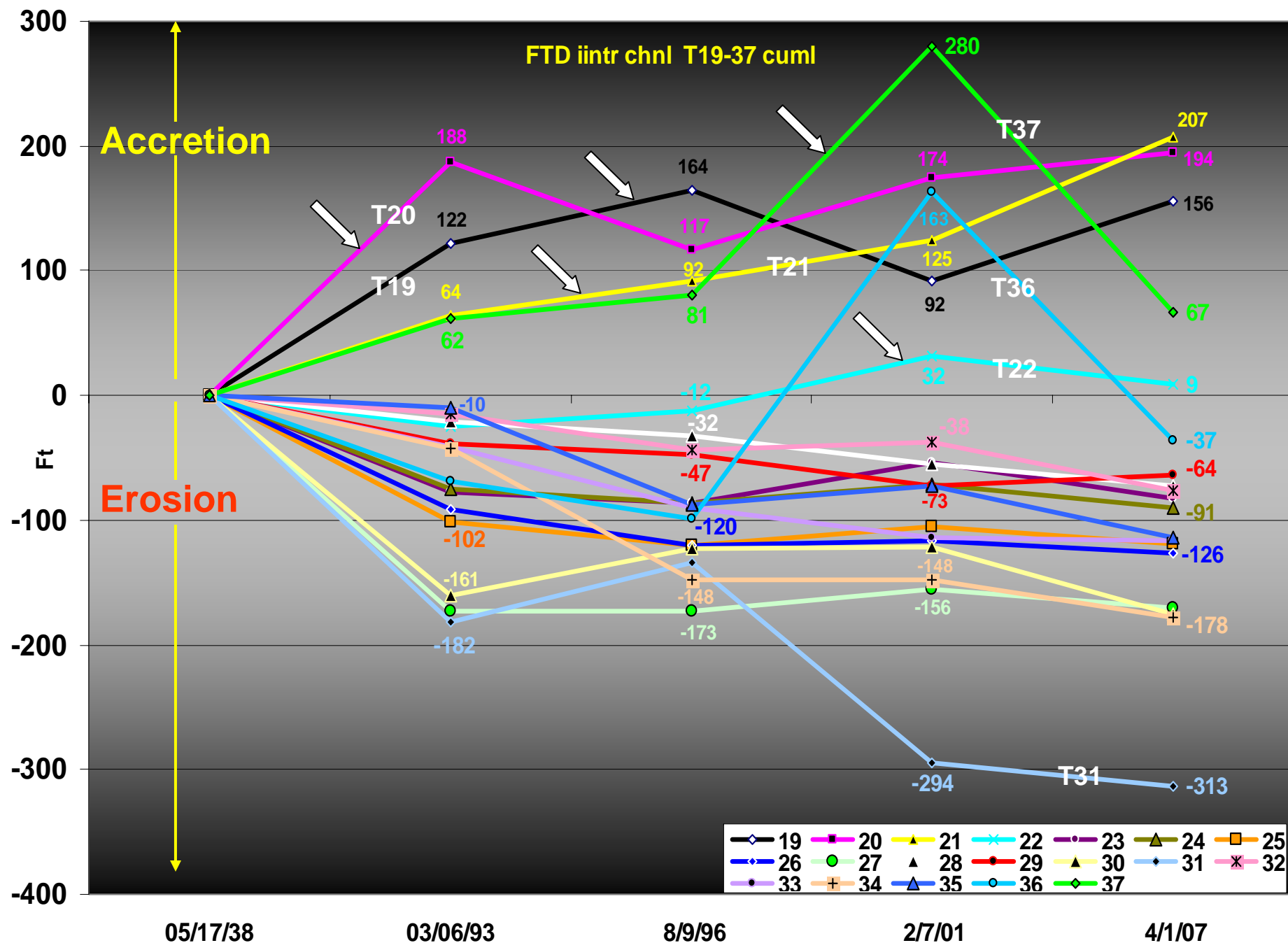


**Figure 46.** Graph depicting the cumulative shoreline change along Green and Nixon Channel's interior (landward) margin. Note X axis is not to scale. See Figure 36 for location of transects along flood tidal delta margin. White arrows represent transects where net accretion has occurred.



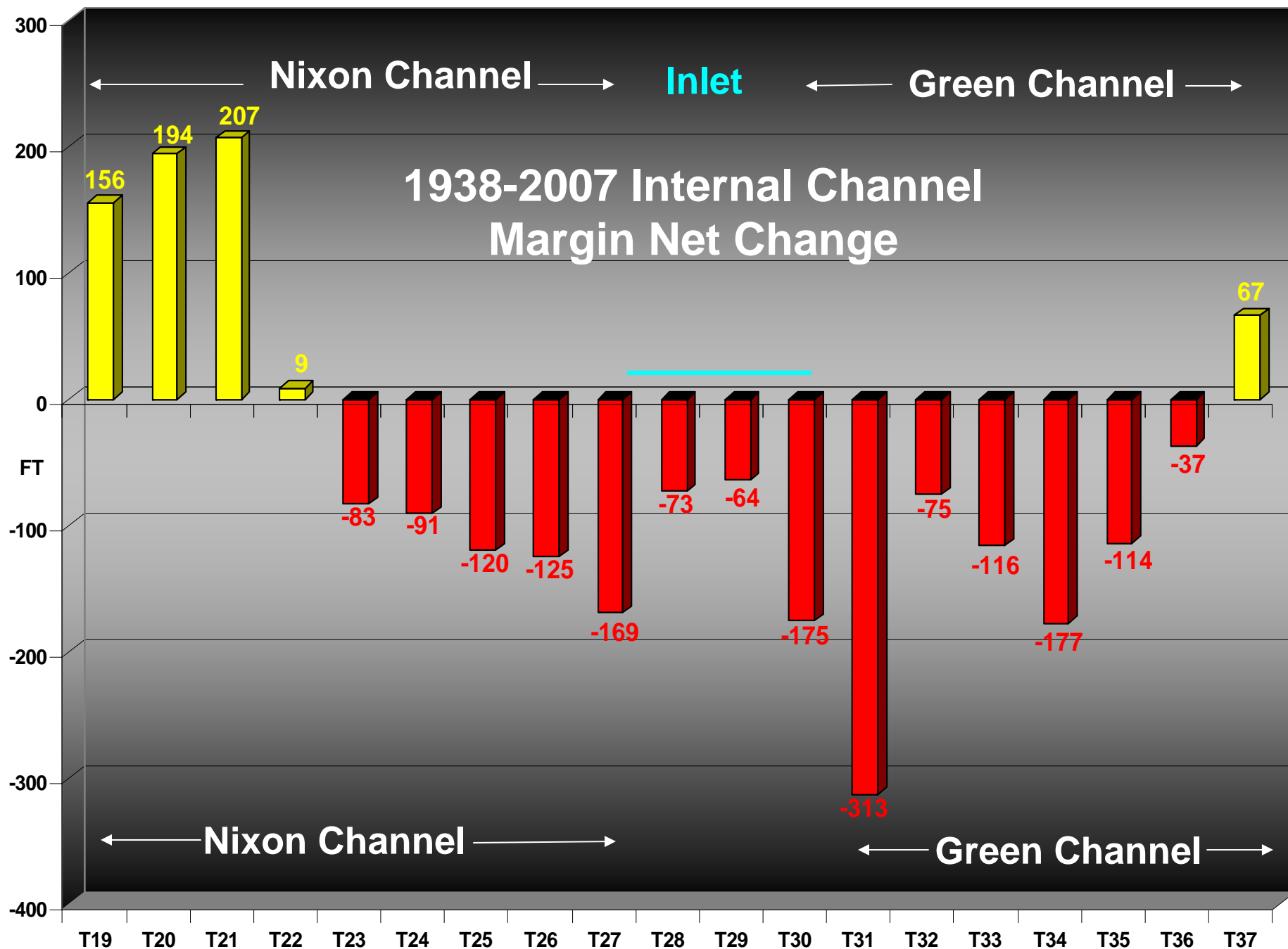


**Figure 47.** Bar graph illustrating net shoreline change along the internal channel margin reach between T19 and T37 during the period from 1938-2007. See Figure 36 for transect locations

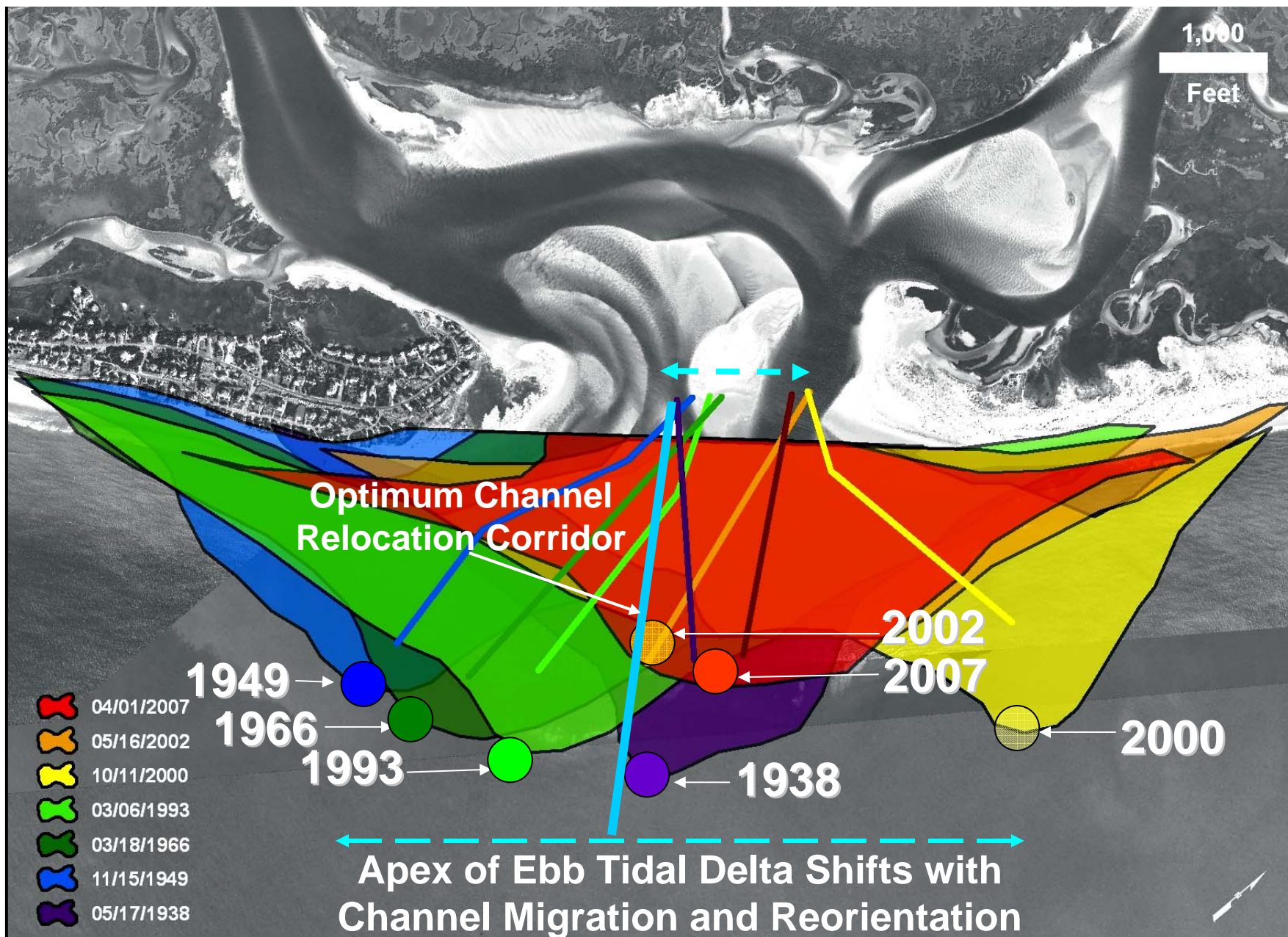


**Figure 48.** Aerial photograph (2007) of Rich Inlet depicting the shapes of various ebb tidal deltas and ebb channel positions for selected years between 1938 and 2007. Colored circles represent the ebb delta apex.



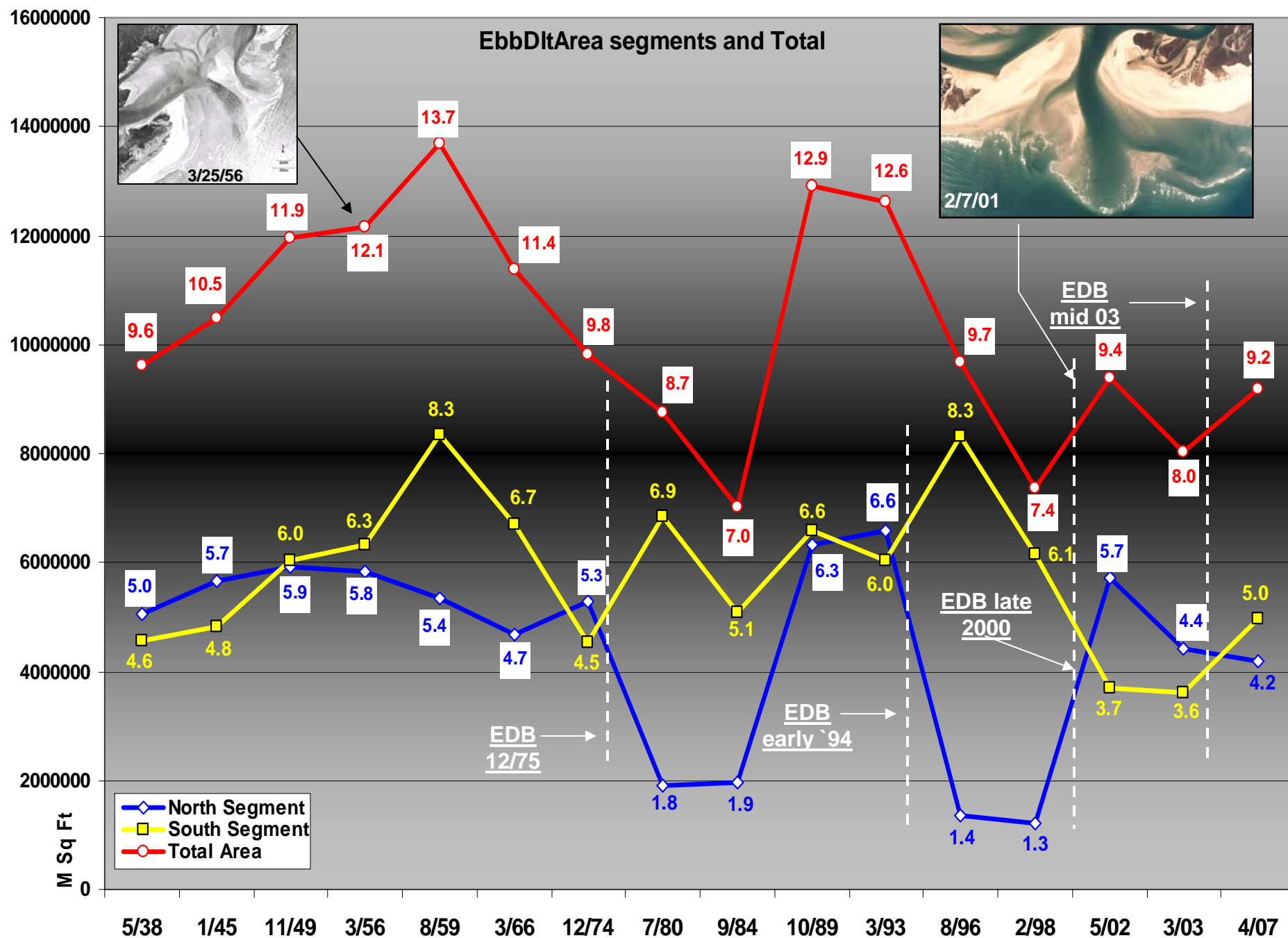


**Figure 49.** Graph depicting the area of the ebb delta segments (A [North] and B [South]) and total ebb-tidal area in millions of square feet (Sq. Ft.) since 1938. Ebb delta breaching events (EDB) are referenced by dashed white colored lines.

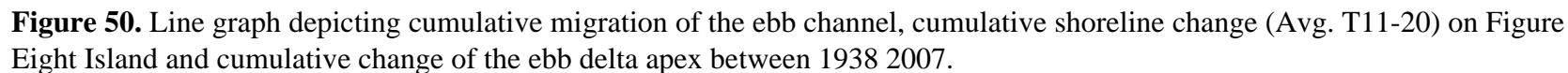


**Figure 50.** Line graph depicting cumulative migration of the ebb channel, cumulative shoreline change (Avg. T11-20) on Figure Eight Island and cumulative change of the ebb delta apex between 1938-2007.



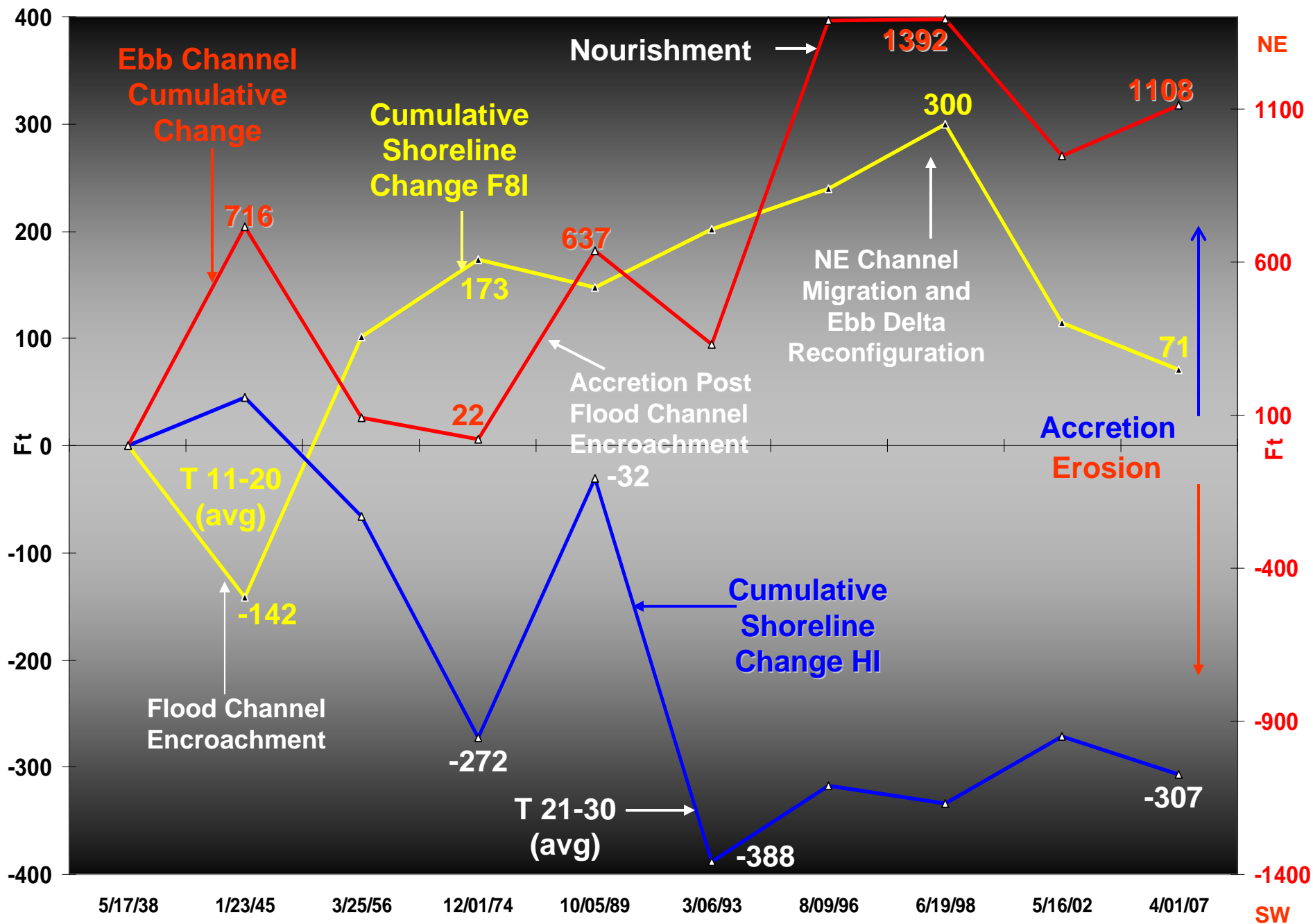


**Figure 51.** Graph comparing F8I and HI cumulative average oceanfront shoreline change (inlet-influenced reach) and ebb channel mid-point migration.





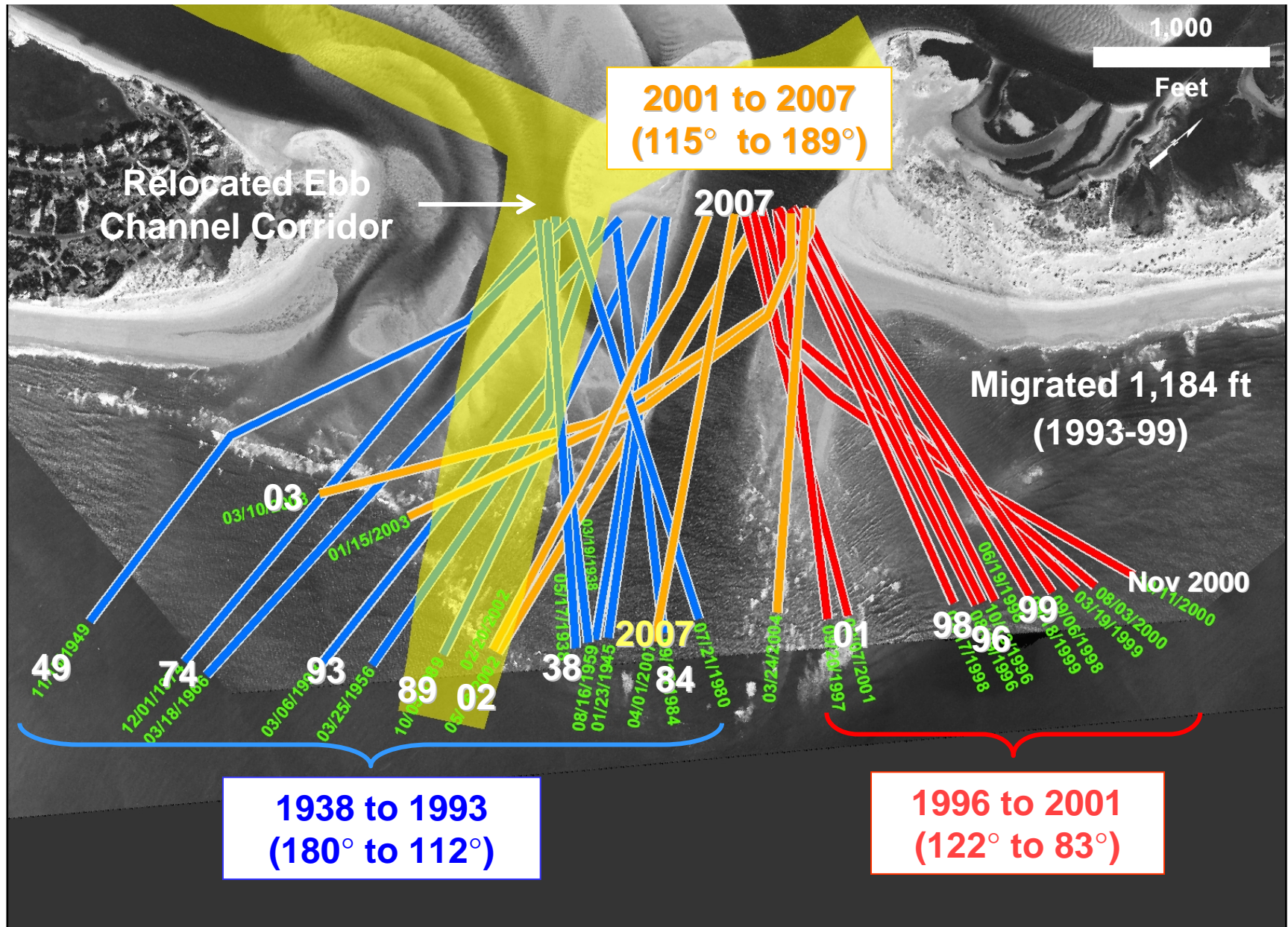


**Figure 53.** Aerial photograph mosaic (2006) depicting position and alignment of the ebb channel between 1938 and 2007. The yellow polygon represents the proposed ebb channel relocation corridor. The proposed channel relocation site represents the most advantageous position and alignment that will promote accretion along the F8I oceanfront shoreline.



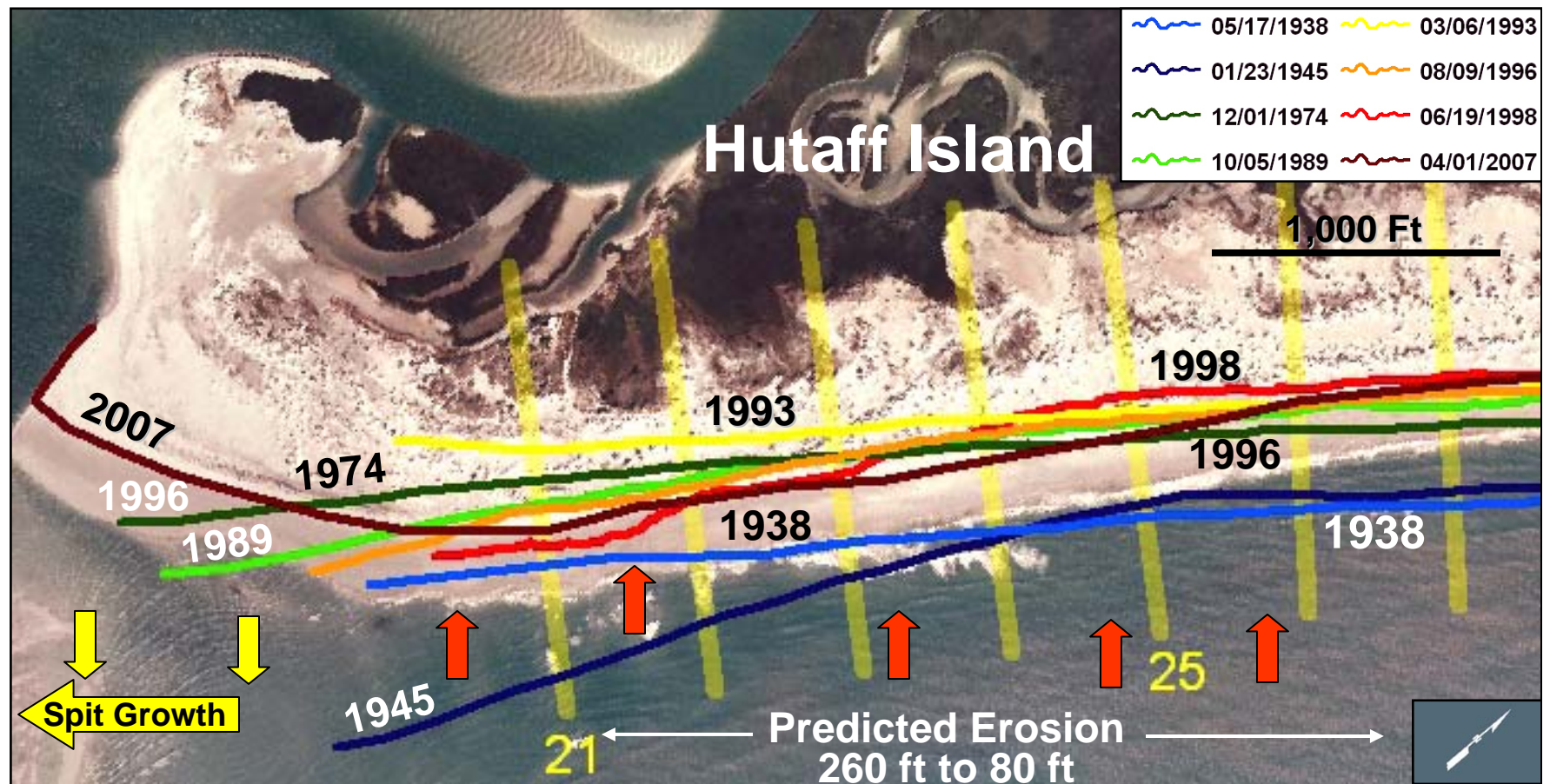


**Figure 54.** Map depicting the various positions of historic shorelines along the Hutaff Island oceanfront between 1938 and 2007. Note the position of 1945 shoreline. Channel relocation will induce erosion along the shoreline segment between T21 –T27 and concurrently will promote island lengthening thru spit growth. Base aerial photograph dates from 2007.